Modeling Spatio-Temporal Pattern of Drought Using Three-Dimensional Markov Random Field

Virat Shukla

January, 2007

Modeling Spatio-Temporal Pattern of Drought Using Three-Dimensional Markov Random Field

by

Virat Shukla

Thesis submitted to the International Institute for Geo-information Science and Earth Observation in partial fulfilment of the requirements for the degree of Master of Science in Geo-information Science and Earth Observation, Specialisation: Geoinformatics.

Thesis Assessment Board

Prof. Dr. Alfred Stein
Dr. V.K. Dadhwal (Dean, IIRS)
Dr. N.R. Patel (IIRS)
C. Jeganathan (Course-Coordinator)
Prof. S.S Hundal (External Examiner)

Thesis Supervisors

Dr. N.R. Patel (IIRS)
Dr. V.A. Tolpekin (ITC)

INTERNATIONAL INSTITUTE FOR GEO-INFORMATION SCIENCE AND EARTH OBSERVATION
ENSCHEDE, THE NETHERLANDS
&
INDIAN INSTITUTE OF REMOTE SENSING, NATIONAL REMOTE SENSING AGENCY (NRSA), DEPARTEMENT OF SPACE, GOVT. OF INDIA, DEHRADUN, INDIA

Disclaimer

This document describes work undertaken as part of a programme of study at the International Institute for Geo-information Science and Earth Observation. All views and opinions expressed therein remain the sole responsibility of the author, and do not necessarily represent those of the institute.

Abstract

Droughts are major natural disasters for many parts of world. Dry areas, where precipitation pattern is markedly seasonal, or is otherwise highly variable, are the most susceptible. Unlike most natural disasters, drought onset is difficult to identify. Meteorological and agricultural drought occurrences along time and space take place randomly and therefore their scientific quantifications are possible by the probabilistic methods. In the present work an effort has been made to derive drought pattern using spatio-temporal information by the use of temporal images from NOAA-AVHRR based Normalized Difference Vegetation Index (NDVI) and meteorological based Standardized Precipitation Index (SPI).

Correlation and regression analysis was performed between Standardized Vegetation Index (SVI) and Standardized Precipitation Index (SPI). On the basis of observed relationship between SPI and SVI on monthly basis, quantification of drought class in terms of data descriptor was done and finally generalized classification of drought class was presented.

In this study we propose a spatio-temporal explicit algorithm called as Three-Dimensional Markov random field model for the identification of drought pattern at next moment of time. This algorithm is based on the assumption that SVI reflects the state of vegetation at the given moment and SPI influences the state of vegetation in the future, this effect was modeled by incorporation of spatio-temporal contextual information in terms of energy function. The algorithm is initialized by the calculation of class temporal prior probability from the temporal images. Finally, an iterative algorithm, Simulated annealing, was used to compute global posterior energy for all possible updates of the class labels and new class label was chosen that correspond to lowest energy value. A difficult issue related to MRF is the determination of the MRF model parameters that weight the energy terms related to the available information sources. The concept of minimum perturbation was used to estimate the parameters value.

The overall methodology presented in this study provides a general framework on the use of spatio-temporal information from NDVI time series data in drought Modeling using Three-Dimensional Markov Random Field Model.

Keywords: Drought, Standardized Vegetation Index, Standardized Precipitation Index, Three-dimensional Markov Random Field, Simulated Annealing, Minimum Perturbation energy.

Acknowledgements

Sometimes “Thanks” are but a humble expression of the deep debt of gratitude which one’s feels in one’s heart but since there is no other word which can better express one’s feeling of gratitude than this. I must have recourse to it and express my deep debt of gratitude to my Supervisor Dr.N.R Patel, Agriculture and Soil Division, IIRS.

Gifted with technical acumen, he has all along been guided me with genial keenness and benign interest. I thank him for his constant support and encouragement. Dr.V.K.Dadhwal, Dean, IIRS, deserves my sincere thanks in this venture of mine.

My special thanks to my ITC supervisor Dr. V.A.Tolpekin, Department of Earth Observation Science, ITC, The Netherlands for his tireless effort and thought put into this research. More importantly, I thank him for all the guidance and support. Whatever little has been done is to a large measure due to his relentless & useful criticism & constructive suggestions from time to time.

Moreover, I would like to show my gratitude to Dr. R. Ramachandran, Dr. Chandrakanth and Dr. Suresh kumar, ADRIN, for their input and support at the final stage of this study. I also thank them for giving me the privilege to work at ADRIN and appreciate the staff and resources associated with this organization.

I take this opportunity to appreciate all my Geoinformatics and Geo-hazards batchmates: Mr. Prashant Kawishwar, Mr. R.R Okhandiar, Vinod, Rajiv, Pankaj, Divyani, Majani, Sreyasi, Chandrama, Mr. Shivraj Godpade, Lesslie and Rajesh for making my stay pleasant and memorable at IIRS and ITC.

I would like to express my special thanks to Anil Rawat for his technical guidance.

Not the least I must thank to my Parents who bore the financial burdens for this work & for their loving and caring support in every aspect of life. Finally, without the blessing of my Mother and brother to provide me with a clear mind and the support of my near and dear one’s none of this would have ever been possible. I cannot express how much you all mean to me.

Table of contents

List of figures

List of tables

1. Introduction

1.1. Drought

Drought is complex event which may impair social, economic, agricultural and other activities of society. It is a prolonged, abnormally dry period when there is shortage of water for normal needs. It is temporary, recurring natural disaster, which originates from the lack of precipitation and brings significant economic losses. It is a slow poison, no one knows when it creeps in, it can last any number of days and its severity cannot be predicted. The non-structural characteristic of drought impacts has certainly hindered the development of accurate, reliable, and timely estimates of severity and ultimately, the formulation of drought preparedness plans by most governments. The impacts of drought, like those of other hazards, can be reduced through mitigation and preparedness.

Drought is an extended period where water availability falls below the statistical requirements for a region. It is not a purely physical phenomenon, but rather interplays between natural water availability and human demands for water supply.

There are two main kinds of drought definitions: conceptual and operational. Conceptually, it can be defined as “a protracted period of deficient precipitation resulting in extensive damage to crops, resulting in loss of yield.”(National Drought Mitigation Center,2006). Conceptual definitions may also be important in establishing drought policy. Operational definitions identify the beginning, end, spatial extent and severity of a drought. They are often region-specific and are based on scientific reasoning, which follows the analysis of certain amounts of hydro meteorological information. They are beneficial in developing drought policies, monitoring systems, mitigation strategies and preparedness plans. Operational definitions are formulated in terms of drought indices. It is not possible to avoid droughts. The success of drought preparedness and its impact, amongst the others, on how well the droughts are defined and drought characteristics quantified (Smakhtin and Hughes, 2004).

Defining drought is difficult; it depends on differences in regions, needs, and disciplinary perspectives. Drought always starts with the lack of precipitation, but may (or may not, depending on how long and severe it is) affect soil moisture, streams, groundwater, ecosystems and human beings. This leads to the identification of different types of drought (meteorological, agricultural, hydrological, socio-economic, ecological), which reflect the perspectives of different sectors on water shortages. Figure 1-1 explains these perspectives in a concise manner.

1.1.1. Types of drought

Droughts can be classified in four major categories:
Meteorological drought: It simply implies rainfall deficiency where the precipitation is reduced by more than 25%from normal in any given area. These are region specific, since deficiency of precipitation is highly variable from region to region.

Hydrological drought: These are associated with the deficiency of water on surface or subsurface due to shortfall in precipitation. Although all droughts have their origination from deficiency in precipitation, hydrological drought is mainly concerned about how this deficiency affects components of the hydrological system such as soil moisture, stream flow, ground water and reservoir levels etc.

Agricultural drought: This links various characteristics of meteorological or hydrological drought to agricultural impacts, focusing on precipitation shortages, differences between actual potential evapo-transpiration, soil, soil water deficits, and reduced ground water or reservoir levels. Plant water demand depends on prevailing weather conditions, biological characteristics of the specific plant, and its stage of growth and the physical and biological properties of the soil.

Socio-economic drought: It is associated with the demand and supply aspect of economic goods together with elements of meteorological, hydrological and agricultural drought. This type of drought mainly occurs when there the demand for an economic good exceeds its supply due to weather related shortfall in water supply.

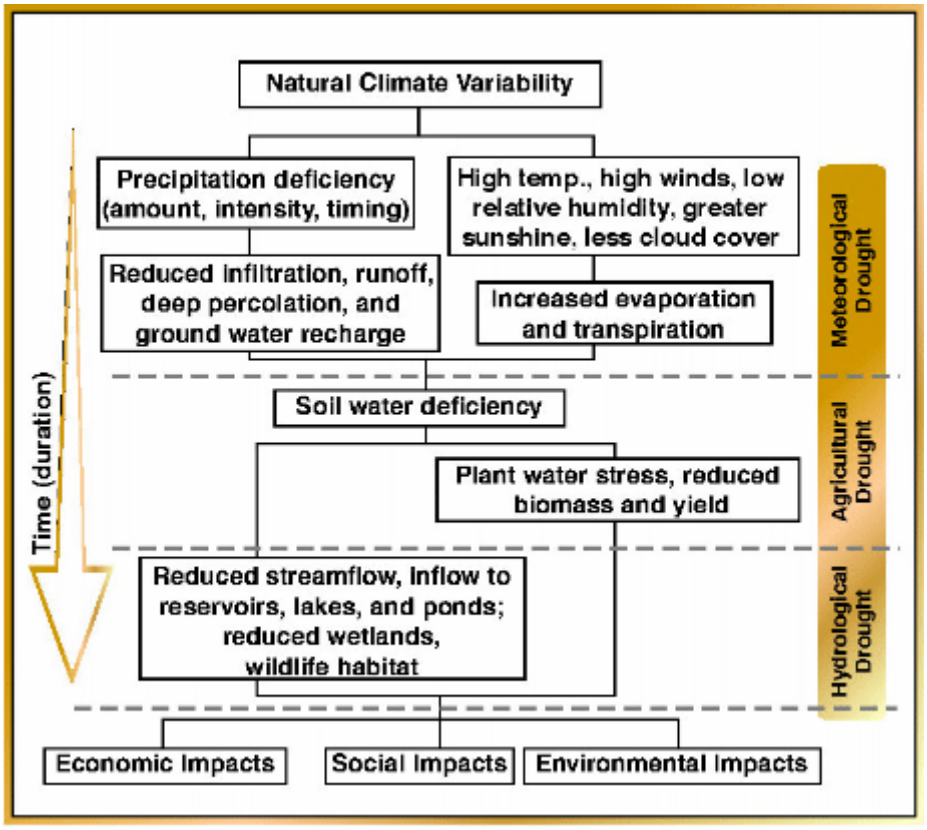

Figure 1-1: Relationship between meteorological, hydrological and agricultural drought

(Source: National Drought Mitigation Centre, http://drought.unl.edu/whatis/concept.htm)

1.1.2. Drought in India

India is predominantly an agrarian country as more than 70% of its population is dependent on agriculture. Rainfall is the main source of water for agriculture. Drought is measured in terms of meteorological drought. It is well known that the supply of water through rainfall cannot be as regular as it can be through irrigation. Almost 20% of the total area of the country lies in the dry farming tract where annual rainfall is between 40 and 100 cm without any irrigation support. Thus even after full exploitation of irrigation potential in the country, it is estimated that about

70 million ha of cultivable land will be under rain fed agriculture, spread over some parts of Haryana, Rajasthan, Uttar Pradesh, Madhya Pradesh, Maharashtra, Gujarat, Andhra Pradesh, Karnataka, and Tamil Nadu. Farmer experiences the worst ill effects of drought. Due to the vagaries of rainfall, more than 68% of the net sown area in the country is drought prone, out of which 50% is severe in nature. The country experiences drought every 2 to 3 years in one part or other.

The drought of 1987 was one of the worst in the country. The drought of 1987 was one of the worst in the century. The monsoon rainfall was normal only in 14 out of 35 meteorological sub-divisions in the country. The overall deficiency in rainfall was 19% as compared to 26% in 1918 and 25% in 1972 being worst years. Agricultural operations were adversely affected in 43% (58.6 million ha) of cropped area in 263 districts in 15 States and 6 Union Territories. In the two worst affected states of Rajasthan and Gujarat, the rainfall was less than 50% from normal. In these states, the drought of 1987 was the third or fourth in succession resulting in distress to an unprecedented level. Gujarat is one such state where drought occurs with unfailing regularity. All India and Gujarat state drought years can be analyzed from Table 1-1.

Table 1-1All India and Gujarat State Drought Years,

1901-1910	1911-1920	1921-1930	1931-1940	1941-1950	1951-1960	1961-1970	1971-1980	1981-1990	1991-2000
Gujarat State									
1901	1911	1923	1931	1942	1951	1962	1972	1982	1991
1904	1915	1924	1936	1948	1952	1963	1973	1985	1993
1905	1918	1925	1938		1955	1965	1974	1986	1995
	1920	1927	1939		1957	1966		1987	1998
		1929	1940		1960	1968		1990	1999
									2000
All India									
1901	1911			1941	1951	1965	1972	1982	
1904	1918					1966	1974	1987	
1905	1920					1968	1979		

Source(Gore and Ponkshe, 2004)

Gujarat is chronically dry and prone to drought. Drought in the state is the result of a combination of natural factors, principally the scarcity of rain, and man-made factors such as deforestation and overgrazing, the absence of traditional rainwater harvesting systems etc. In 1999, as many as 98 out of a total of 225 blocks in the state received less than 50% of the season's expected rainfall. In 1999, Gujarat faced the worst drought of the past 100 years. Some 7,500 villages spread over 145 blocks in 15 districts were severely affected. The state has been hit by the worst drought in 100 years. More than 25 million people living in 9,000 villages of 17 of the 25 districts have been hit. Though Saurashtra has always been drought prone, this year the districts of Jamnagar, Rajkot, Junagadh, Amreli, Bhavnagar, Surendranagar and Porbandar have also been badly affected. Almost all water sources have dried up; there is no food for the people and no fodder for over 7 million cattle. The water table in drought affected Saurashtra, Kutch and northern Gujarat is said to be falling by 10-15 feet each year (Bavadam, 2001).

In India, Department of Agriculture and Cooperation and Department of Space sponsored the remote sensing application mission on drought, which is being executed by National Remote Sensing Agency with participation by Indian Meteorological Department (IMD), Central Water Commission (CWC) and concerned state government agencies. The focus is on assessment of agricultural drought conditions. The project leads to the development of National Agricultural Drought Assessment and Monitoring System (NADAMS). NADAMS used fortnightly NDVI images derived from NOAA-AVHRR during its first phase to assess drought in a district level with a turn around time of less than two days. The second phase attempted sub district level monitoring and the current phase uses high-resolution satellite data for crop specific and comprehensive monitoring.

1.2. Markov Random Field to identify drought

As the drought conditions creep into the system at a slow rate, the prescription for drought management (before, during and after the event) include: - on-set identification, status of intensity, mitigation measures for re-orientation or change and information dissemination activities. This requires an understanding of the past events and comparison with the present day conditions. The voluminous information is available in the form of text, analogue, numerical and graphics representing the spatial and temporal situations. Thus it is necessary to handle historical datasets to study the spatio-temporal pattern of drought in order to predict the drought conditions. A required degree of relationship has to be made between large numbers of NDVI images and rainfall datasets for efficient prediction; we propose to utilize the techniques such as three-dimensional Markov random field.

Drought characteristics of any phenomenon are dependent on the underlying generating mechanism and can be modelled by suitable technique. In interpretation of drought condition, context is very important. It may be derived from spectral, spatial or even temporal attributes. Using concept of context, pixel in the image are not treated in isolation, but are considered to have relationship with their neighbours. Thus the relationship between pixel of interest and its neighbours is treated as being statistically dependent. A nearest neighbourhood dependence of pixels on an image lattice is obtained by going beyond the assumption of statistical independence. Information on the nearest neighbourhoods is used to calculate conditional probabilities. Contextual information can be integrated for image analysis by using Markov Random Field (Li, 2001; Tso and Mather, 2001). MRF theory is a branch of probability theory for analyzing the spatial or contextual dependencies of different phenomena. Various MRF models have been widely employed for image processing which include image restoration and segmentation, surface reconstruction, edge detection, texture analysis and so on (Li, 2001).

The Markov chain approach is a statistical technique used to predict precipitation on short term at meteorological stations. This approach has two advantage; one is that the forecasts are available immediately after the observations are done because they use only local information on the weather for prediction and secondly they need minimal computation after the climatological data has been processed. Two criteria are use to decide among different orders of the Markov chain models: the Akaike criterion and Bayesian criterion (BIC). Both are based on the loglikelihood functions for the transition probabilities of the Markov chains constructed on a certain data series. Normally, the BIC criterion values have been calculated based on transition and it has been found that first-order Markov chain is the best representation for the daily

precipitation occurrence. Hess et al. have demonstrated that this technique is good enough to build an objective base of the precipitation occurrence probability in short-term prognosis (Cazacioc and Cipu, 2004). A first-order Markov chain approach can be used for monitoring drought as it need only one variable (like cloudiness, precipitation amount, temperature, fog, wind) at a given time which is sufficient to forecast it at some later time. It can be applied to the time series of daily precipitation. Incorporating spatial-temporal aspect, this study aims at studying the spatio-temporal variation of drought patterns and drought severity using three-dimensional Markov random field.

1.3. Drought indices

Drought indices assimilate thousands of bits of data on rainfall, snow pack, stream flow, and other water supply indicators into a comprehensible big picture. A drought index value is typically a single number, far more useful than raw data for decision making (Hayes and Michael, 2006). Drought indices can be derived from hydro-meteorological data and remote sensing data.

1.3.1. Drought Indices derived from Hydro-meteorological data

Drought indices are normally continuous functions of rainfall and/or temperature, river discharge or other measurable variable. Rainfall data are widely used to calculate drought indices, because long-term rainfall records are often available. Rainfall data alone may not reflect the spectrum of drought related conditions, but they can serve as a pragmatic solution in data-poor regions. Hydro meteorological data based indices include Palmer Drought Severity Index (PDSI), Bhalme-Mooley Drought Index (BDMI), Crop Moisture Index (CMI), Agro-Hydro Potential (AHP), Standardized Precipitation Index (SPI), Surface Water Supply Index (SWSI), Reclamation Drought Index (RDI), Deciles etc. Among the aforementioned indices SPI is used for this research work.

1.3.1.1. Standardized Precipitation Index (SPI)

(McKee et al., 1993) of the Colorado Climate Centre formulated the SPI in 1993. The purpose is to assign a single numeric value to the precipitation that can be compared across regions with markedly different climates. Technically, the SPI is the number of standard deviations that the observed value would deviate from the long-term mean, for a normally distributed random variable. Since precipitation is not normally distributed, a transformation is first applied so that the transformed precipitation values follow a normal distribution.

The SPI was designed to quantify the precipitation deficit for multiple time scales. These time scales reflect the impact of drought on the availability of the different water resources. Soil moisture conditions respond to precipitation anomalies on a relatively short scale while groundwater, stream flow, and reservoir storage reflect the longer-term precipitation anomalies. Thus, (McKee et al., 1993) originally calculated the SPI for 3, 6, 12, 24, and 48 month time scales.

The SPI calculation for any location is based on the long-term precipitation record that is fitted to a probability distribution, which is then transformed into a normal distribution so that the mean SPI for the location and desired period is zero (Edwards et al., 1997). A drought event

occurs any time the SPI is continuously negative and reaches intensity of -1.0 or less. The event ends when the SPI becomes positive. Each drought event, therefore, has a duration defined by its beginning and end, and intensity for each month that the event continues. The positive sum of the SPI for all the months within a drought event can be termed the drought's "magnitude".

Table 1-2 Standardized Precipitation Index

SPI VALUES	
2.0+	Extremely wet
1.5 to 1.99	Very wet
1.0 to 1.49	Moderately wet
-0.99 to 0.99	Near normal
-1.0 to -1.49	Moderately dry
-1.5 to -1.99	Severely dry
-2 to less	Extremely dry

(Source: http://drought.unl.edu/monitor/spi)

1.3.2. Satellite based drought indices

Satellite data in drought monitoring has long been proven and needs no iteration. Drought indicators assimilate information on rainfall, stored soil moisture or water supply but do not express much local spatial detail. Also, drought indices calculated at one location is only valid for single location. Thus, a major drawback of climate based drought indicators is their lack of spatial detail as well as they are dependent on data collected at weather stations which sometimes are sparsely distributed affecting the reliability of the drought indices (Brown et al., 2002). Satellite derived drought indicators calculated from satellite-derived surface parameters have been widely used to study droughts. Normalized Difference Vegetation Index (NDVI) and Standardized Vegetation Index (SVI) are vegetation indices used in this study.

1.3.2.1. Normalized difference vegetation index (NDVI):

Tucker first suggested NDVI in 1979 as an index of vegetation health and density (Thenkabail et al., 2004). NDVI is defined as:

$$NDVI = \frac{(\lambda_{NIR} - \lambda_{RED})}{(\lambda_{NIR} + \lambda_{RED})} \qquad \textbf{Equation 1-1}$$

Where, λ_{NIR} and λ_{RED} are the reflectance in the NIR and red bands, respectively. NDVI is a good indicator of green biomass, leaf area index, and patterns of production (Thenkabail et al., 2004; Wan et al., 2004). NDVI is the most commonly used vegetation index. It varies from +1 to -1. Since climate is one of the most important factors affecting vegetation condition, AVHRR-NDVI data have been used to evaluate climatic and environmental changes at regional and global scales (Ji and Peters, 2003; Li et al., 2004; Singh et al., 2003). It can be used not only for accurate description of continental land cover, vegetation classification and vegetation vigour but is also effective for monitoring rainfall and drought, estimating net primary production of vegetation, crop growth conditions and crop yields, detecting weather impacts and other events important for agriculture, ecology and economics (Singh et al., 2003). NDVI has been used

successfully to identify stressed and damaged crops and pastures but only in homogenous terrain. In more heterogeneous terrain regions their interpretation becomes more difficult (Jurgen et al., 1998; Singh et al., 2003). Many studies in the Sahel Zone (Anyamba and Tucker, 2005), Mediterranean (Jurgen et al., 1998), and Senegal (Li et al., 2004) indicate meaningful direct relationships between NDVI derived from NOAA AVHRR satellites, rainfall and vegetation cover and biomass.

1.3.2.2. Standardized vegetation index

The Standard Vegetation Index (SVI) is based on the fact that vegetation conditions are closely linked to weather conditions in the atmosphere closest to the ground (Peters et al., 2002). It shows us the effects of climate on vegetation over short-time periods. The values of the SVI range between greater than zero and less than one. "Zero" is the condition in which a pixel NDVI value is lower than all possible NDVI values for a pixel for a month in all other years. The value "one" is the condition in which the pixel NDVI value for the respective month is higher than all the NDVI values of the same month in the other years. One key to interpreting SVI data is to remember that each pixel is being compared only to the data found in that single pixel over time. Comparisons can be made with surrounding pixels but keep in mind that each pixel is being generated only by the data found in that pixel through many years of data.

1.4. Problem Statement

Through their socio-economic impacts on affected areas, droughts are recognized as such when they become natural disasters. However, they differ from most other natural disasters because their recurrence in drought-prone areas every few years is practically certain. They also differ by lacking sudden and easily identified onsets and termination. Droughts vary widely in degree of severity, duration and aerial extent. In order to predict the drought conditions at next moment of time one can use the spatial NDVI images and rainfall datasets. Incorporating spatial-temporal aspect, this study aims at studying the spatio-temporal variation of drought patterns and drought severity using three-dimensional Markov random field. Once an efficient tool is built for prediction of drought, it will enable earth scientists, agriculturists and planners to utilize the same for effective drought mitigation and management.

1.5. Research objective

The general objective of the research is to build a tool for identification of spatio-temporal pattern of drought using Three-dimensional Markov random field.

The outcome of this research provides the users with guidelines on the parameters setting of the Markov random field model. The result obtained using Three-dimensional Markov random field encourages the end users to apply the technique in remotely sensed image with respect to spatio-temporal aspect of the drought to provide more meaningful and understandable information. This kind of information is essential for a broad group of users within the geo-informatics society who are interested in monitoring, mitigation and management of drought.

1.6. Research question

- How to quantify drought classes using NDVI and rainfall datasets in terms of data descriptor?
- How to incorporate NDVI and rainfall datasets in three-dimensional Markov Random field?
- Which method should be used for parameter estimation of three-Dimensional Markov random field model?

1.7. Structure of the thesis:

This thesis contains six chapters. The first chapter highlights the background, objectives and questions of the research. Chapter two gives detailed description of the study area. Chapter three covers previous research carried out in the field of drought monitoring as well as role of remote sensing and GIS technology in the arena of monitoring and prediction of droughts so far. This chapter also includes about the role of Markov Random Field In remote sensing. Chapter four describes the different datasets used for the research and explains the method considered in order to achieve the research objective. Chapter five presents analysis of long-term SVI temporal images as well as SPI to arrive at pattern of drought by incorporating spatio-temporal information using Three-dimensional Markov Random field Model. The ancillary data and meteorological data used helps in determining the meteorological drought. Both these type of droughts are then combined to arrive at model arising out of combined drought. Also chapter describes about the results obtained after the analysis has been done. It covers description of the relationship established between rainfall and vegetation as well as correlation between SPI and SVI. Chapter six draws conclusion of this study and gives recommendation for further research.

2. Study Area

2.1. Location and Extent of study area

Gujarat is situated on the western coast of India between 20º06' to24º42' north latitudes and 68º10'N to 74º28' east longitudes Figure 2-1. It comprises of 25 districts with a total geographical area of 1.96 lakh square kilometres. Gujarat shares a boundary with Rajasthan in the north east, Madhya Pradesh in the east and Maharashtra in the south and south east. It has a 1600 km long coast-line. Its northern boundary forms the international boundary with Pakistan.

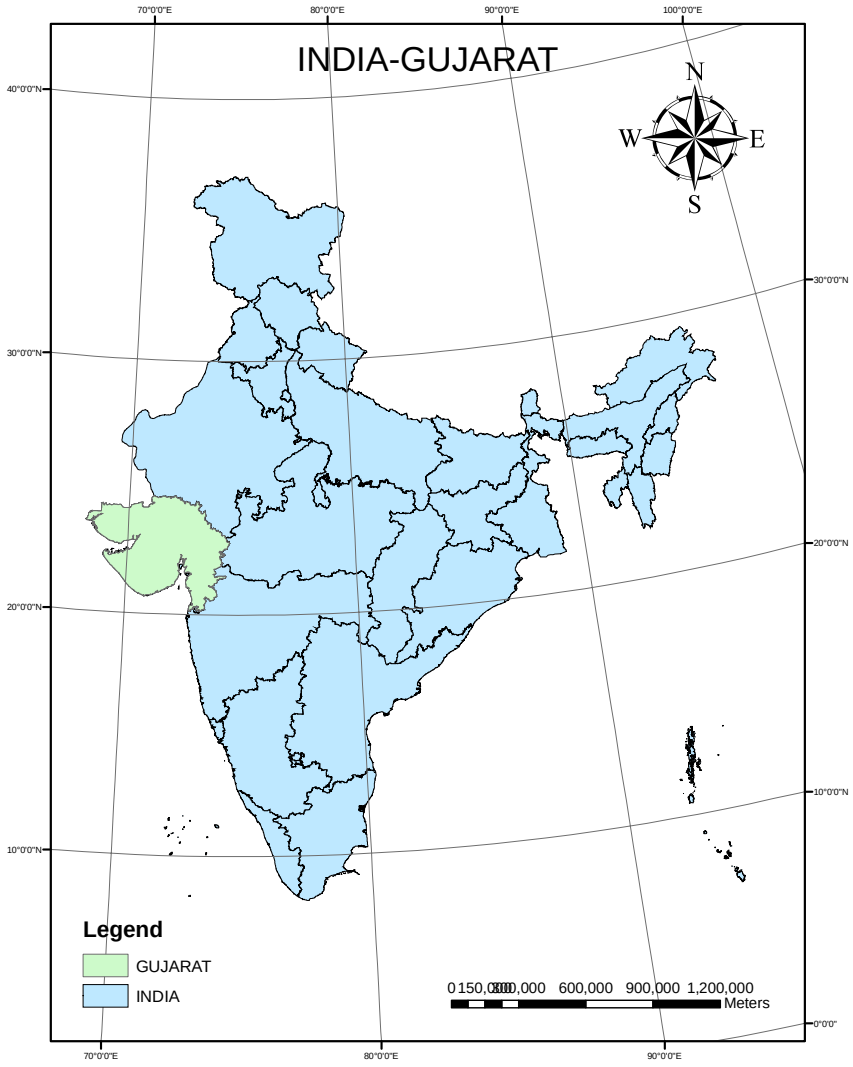

Figure 2-1 Map of India highlighting Gujarat State

2.2. Topography and Drainage

Characterized by a varied topography, Gujarat has a fertile plain in the south cut by several rivers, low hills in the west and broad mudflats in the north that adjoing the Thar (Great Indian) Desert. The Gujarat state has been divided into three major physiographic regions, namely the Central Highlands, the Western Hills and the West Coast. The extreme part of the state is occupied by the Central Highlands, a wide belt of hilly region bordered by the Arravali Range on the west. The Western Hills forms the part of the peninsular plateau while the Western Coast covers major portion of the state, comprising of Gujarat Plain, Kathiawar Peninsula and Kutch Peninsula. Deltaic plains by the alluvium laid by the Tapi, Narmada, Mahi, Sabarmati, Banas and Luni river systems have lead to the formation of Gujarat Plains progressively. Kathiawar Peninsula is a dissected basaltic plateau with flat-topped hills of Mesozoic sandstones in the northeast while the central part forms a high plateau bordered by scarps and dotted hills. The Kutch Peninsula comprises a central high plateau surrounded by dissected scarps and flat-topped mesas on all sides except in the east. The Rann of Kutch is a depositional plain of salt, sand and mud, marked with scattered islands. (NBSS & LUP)

2.3. Climate

The climate of Gujarat is also varied and can be divided into three seasons: (1) hot and dry season from May to June; (2) warm and rainy season from June to September; and (3) cool and dry post-rainy season from October to April (Agro climatology of Gujarat). The north-western part of the state is dry, with less than 500 mm of rain every year. In the more temperate central part of the state, the annual rainfall is more than 700 mm. In the southern part, rainfall averages 2000 mm a year. Incidence and distribution of rainfall, particularly in Saurashtra and Kutch regions and in the northern part of Gujarat is highly erratic. As a result, these regions are very often subjected to drought. Most of the rain (90-95% of the annual total) falls during the period of June to September, when the southwest monsoon prevails. The north- west monsoon does not occur in Gujarat state. In the winter temperatures averages between 12º and 27º. In the summer temperatures average between 25º and 43º and have been known to reach as high as 48ºC. The highest temperatures have been recorded at Ahmedabad and in regions of Banaskantha while temperatures are relatively low at places located in coastal regions.

2.4. Soils

Soils are one of the most valuable life supporting natural resources for the society since they produce food, fiber and fodder, which are basic to our existence. Gujarat is endowed with a wide range of soil type. The soils of Gujarat can be broadly classified into nine groups namely, black soils, mixed red and black soils, residual sandy soils, alluvial soils, saline/alkali soils, lateritic soils, hilly soils, desert soils and forest soils.

2.5. Agroclimatic zones of Gujarat

The state is divided into seven agro climatic zones mainly based on amount of rainfall and soil types.

2.5.1. South Gujarat

This zone is a heavy rainfall area with rainfall ranging between 1500 mm and more, with deep black soils. Most of the area is cultivated. Cotton, paddy, sorghum and sugarcane are major

crops grown in this zone. Whole of Dangs district and parts of Surat and Valsad districts comes under this agro climatic zone.

2.5.2. Middle Gujarat

This zone has rainfall ranging between 800-1000 mm. It consists of Panchmahals, Vadodara and Bharuch districts. Cotton, tobacco, bajra, pulses, wheat, paddy, maize, jowar and sugarcane are major crops.

2.5.3. North Gujarat

It includes whole of Sabarkantha district, parts of Ahmedabad and Banaskantha district, Mehsana and Kheda districts. Rainfall ranges between 625-875 mm. Paddy, bajra, pulse, cotton, groundnut, tobacco, wheat, jowar, millet, vegetables, spices and oil seeds.

2.5.4. Bhal and Coastal area

This zone is comprised of area around gulf of Khambhat and Bhal coastal region in Bharuch and Surat districts. The soils here are poorly drained and saline. Rainfall ranges from 625-1000 mm. Groundnut, cotton, bajra, wheat, pulses and jowar are the major crops grown.

2.5.5. South Saurashtra

Entire of Junagadh district and parts of Bhavnagar, Amreli and Rajkot districts forms this zone. Soils found here are shallow medium black and calcareous. Rainfall ranges between 625-750 mm. Groundnut, cotton and pulses are major cops.

2.5.6. North Saurashtra

Whole of Jamnagar and parts of Rajkot, Surendranagar and Bhavnagar districts make this zone with shallow medium black soils. Rainfall varies between 400-700 mm. Major crops cultivated in this zone comprise of cotton, groundnut, wheat, jowar, and bajra.

2.5.7. North West Zone

The North West zone comprises of entire Kutch, parts of Rajkot, Mehsana, Banaskantha and Ahmedabad districts. Soils in these regions are sandy and saline. Rainfall ranges between 250 - 500 mm. Cotton, sorghum, groundnut, pearl millet and wheat are major crops grown.

2.5.8. Water Resources

Gujarat has 2.28% of India's water resources and 6.39% of country's geographical area (Gupta, 2000). A large percentage of water is consumed by the agricultural sector, for irrigation. Water resources in Gujarat are mainly concentrated in the southern and central part. Saurashtra and Kutch in the northern part, with exceptionally high irrigation needs, have limited surface and groundwater resources. Groundwater has contributed to more than 80% of irrigation in the state .This excessive groundwater mining has thereby reduced the water table by 3-4 cm per year. The depletion of ground water level manifests itself in a fall in the level of water table and an increase in salinity and fluoride content. The fall in ground water levels is a direct result of the rampant use of bore wells, which go as deep as 1,200 feet (360 meters). Water in more than 10,000 wells in Kutch is saline. Though Kutch and northern Gujarat receive low rainfall, these areas have a good aquifer system whereas southern Gujarat, which gets good amount of rainfall, has a poor aquifer system (Bavadam, 2001). Due to typical water-intensive crop varieties, water

surplus areas of south and central Gujarat have also experienced a severe loss of utilizable groundwater as compared to water scarce regions.

2.5.8.1. Land use and Agriculture

Landuse is one of the driving forces behind water demand and critical factors of agricultural drought vulnerability. Agriculture in Gujarat forms a vital sector of the states economy. In Gujarat, about 50% of the area is under cultivation of which only one-fifth is irrigated. About 10% is under forests and the remaining is either left barren or uncultivable waste. A generalised landuse/cover map has been generated with four major classes as rainfed crops, irrigated crops, forest and non-vegetation Figure 2-2. Unsuitable climatic conditions in some parts and rocky terrain with thin or no soils in others, have limited the area suitable for cultivation. State's agriculture productivity fluctuates due to poor soils, inadequate rainfall, frequent droughts and floods, bad drainage and undeveloped irrigation facilities. The state's cropping pattern is unproportionately dominated by cash crops. Gujarat is the highest producer of cotton in the country claiming the best agricultural land. The state produces a large variety of crops namely groundnut (highest production in the country), tobacco (second highest production in the country), and isabgul, cumin, sugarcane, jawar, bajra, rice, wheat, pulses, tur and gram which are important crops of Gujarat.

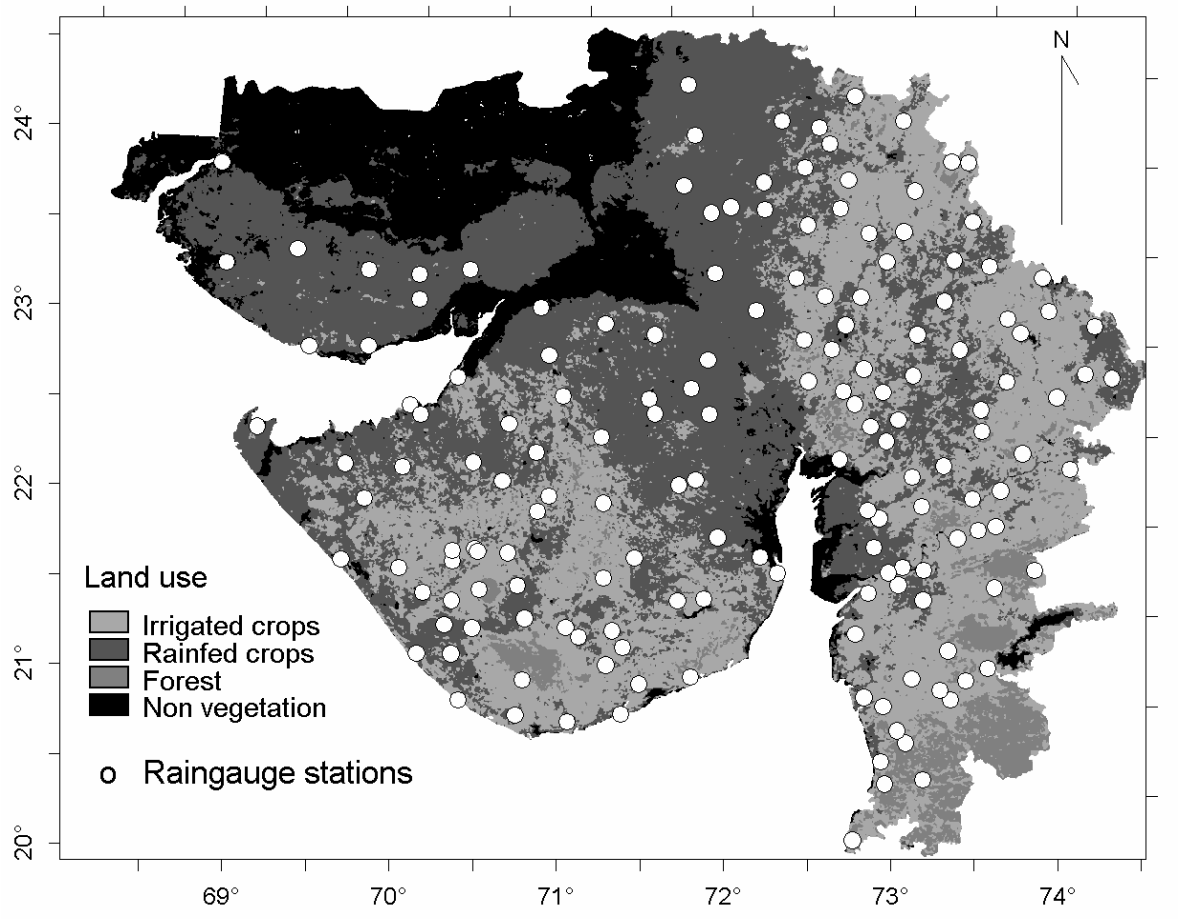

Figure 2-2 Study area showing land use and location of rain gauge stations

3. Literature Review

3.1. Drought assessment: Remote sensing and meterological drought indices

Natural disasters are inevitable and it is almost impossible to fully recoup the damage caused by the disasters. But it is possible to minimise the potential risk by developing disaster early warning strategies, prepare and implement developmental plans to provide resilience to such disasters and to help in rehabilitation and post disaster reduction. Space technology plays a crucial role in efficient mitigation and management of disasters.

Remote Sensing and GIS in Disaster Management Mitigation of natural disaster management can be successful only when detailed knowledge is obtained about the expected frequency, character, and magnitude of hazard events in an area. Although, natural disaster have shown in the last decades a drastic increase in magnitude and frequency, it can as be observed that there is a dramatic increase in technical capabilities to mitigate them.

We now have access to information gathering and organizing technologies like remote sensing and GIS, which have proven their usefulness in disaster management. Remote sensing and GIS provides a data base from which the evidence left behind by disaster that have occurred before can be interpreted, and combine with the other information to arrive at hazard maps, indicating which area is potentially dangerous. Using remote sensing data, such as satellite imageries and Arial photos, allows us to map the variability's of terrain properties, such as vegetation, water, geology, both in space and time. Satellite images give a synoptic overview and provide very useful environmental information, for a wide range of scales, from entire continents to detail of a few meters. Many types of disasters, such as floods, droughts, cyclones, volcanic eruptions, etc. will have certain precursors that satellite can detect. Remote sensing also allows monitoring the event during the time of occurrence while the forces are in full swing. The vantage position of satellite makes it ideal for us to think of, plan for and operationally monitor the event.

The impact of drought on society and agriculture is a real issue but it is not easily quantified. Reliable indices to detect the spatial and temporal dimensions of drought occurrences and its intensity are necessary to assess the impact and also for decision-making and crop research priorities for alleviation (Seiler et al., 1998). The development and advancements in space technology, to address issues like drought detection, monitoring and assessment have been dealt with very successfully and helped in formulation of plans to deal with this slow onset disaster. With the help of environmental satellite, drought can be detected 4-6 weeks earlier than before and delineated more accurately, and its impact on agriculture can be diagnosed far in advance of harvest, which is the most vital for global food security and trade(Kogan, 1990).

Several indices have been developed for the quantification of drought based on the type of drought. With the advancements in remote sensing technology, the historical drought indices were over powered by the newly developed indices from remote sensing data that are considered

to be real time. Also, the remote sensing has provided a complete coverage of extended regions with a spatial resolution of a few hundred meters to few kilometres. Thus, for an accurate assessment of the occurrence extent and severity drought it is necessary to get a correct picture of the spatial and temporal distribution of a number of meteorological, hydrological and surface variables. Space observation having this potential has made a significant contribution in this field. The satellite sensors that have the capability to retrieve surface parameters with high spatial and temporal resolutions over large areas have provided a comprehensive view of the situation. Many drought studies have made an extensive use of the AVHRR derived data, as it monitors earth surface changes continuously, freely accessible and moreover it's widely recognized around the world.

Drought indices have been developed as a means to measure drought. Some of the widely used drought indices include Palmer Drought Severity Index (PDSI), Crop Moisture Index (CMI), Standardized Precipitation Index (SPI), Surface Water Supply Index (SWSI) and Standardized Vegetation Index (SVI).

(Hayes et al., 1999), used the Standardized Precipitation Index (SPI) to monitor the 1996 drought in the United States of America.. (Hayes et al., 1999), shown that the onset of the drought in the USA in 1996 could have been detected one month in advance of the Palmer Drought Severity Index (PSDI).

Using SPI index one can develop climatology of the spatial extension and intensity of droughts which provides additional understanding of its characteristics and an indication of the probability of recurrence of drought at various levels of severity.

(Ji and Peters, 2003) undertook a study relating to assessing vegetation response in the northern Great Plains using vegetation and drought indices. The study focused on three major areas namely relationship between NDVI and SPI at different time scales, response of NDVI to SPI during different time periods within a growing season and regional characteristics of the NDVI-SPI relationship. It was found that the 3- month SPI has the highest correlation to the NDVI, because the 3- month SPI is best for determining drought severity and duration. Also it was found that seasonality has a very significant effect on the relationship between the NDVI and SPI.

Recent research has shown that the SPI has many advantages over the PDSI and other indices in that it is relatively simple, spatially consistent, and temporally flexible, thus allowing observation of water deficits at different scales (Hayes et al., 1999). Therefore, SPI can be used as reliable agent for detecting emerging drought and important tool for assessing moisture condition and initiating mitigation and response actions.

Seasonal timing of measurements is an important factor in the understanding of vegetation vigour and precipitation relationships, and should be taken into account. Recently, (Peters et al., 2002) described the Standardized Vegetation Index (SVI), which is calculated using a Z score and converted to a probability value to evaluate vegetation and drought status with in growing season.

Using NOAA Advanced Very High Resolution Radiometer (AVHRR) data, researchers have successfully extended satellite data analysis to large-area vegetation monitoring (Kogan, 1990). Since vegetation indices derived from the AVHRR sensor are directly related to plant vigour, density, and growth conditions, they may also be used to detect unfavourable environmental variables. The relationship between NDVI and rainfall is known to vary spatially, notably due to the effects of variation in properties such as vegetation type and soil background (Ji and Peters, 2003) with the sensitivity of NDVI values to fluctuations in rainfall, therefore, varying regionally.

Because of the close relationship between vegetation vigour and available soil moisture, especially in arid and semiarid areas, the AVHRR-derived NDVI has been used to evaluate drought condition by directly comparing it to precipitation or drought indices (Tucker, 1989).To make the NDVI comparable among dates, geographic locations and vegetation types, it has been standardized on the basis of relative values. The use of NDVI-based indices for monitoring and detecting drought is justified on the basis that vegetation vigour is closely related to moisture condition.

3.2. Probabilistic Drought characterization

Forecasting of when a drought is likely to begin or to come to an end is extremely difficult .A better characterization of droughts through drought indices is essential to support appropriate monitoring and prediction tools, which allow for drought warning. The Markov chain approach was used by (Lohani and Loganathan, 1997) and (Lohani et al., 1998) to develop an early warning tool. These authors adopted a non-homogeneous Markov chain formulation to derive drought characteristics and assess dry spells from long-term records of the PDSI in two climatic areas of Virginia (USA). Monthly values of the PDSI for the period 1895–1990 were used. The PDSI values were grouped in seven classes, from the wettest (PDSI > 4.00) to the driest (PDSI< -4.00), being class 4 the normal precipitation class. The long-term probabilities of drought severity classes, their mean duration and the time to return to a particular drought class were computed and two methods for predicting drought severity classes were developed for 1–3 months lead-time. (Sen, 1998) proposed two probabilistic models for drought characterization, regional persistence and multiseasonal respectively. They conclude that drought occurrences are dependent on the regional and temporal dry and wet spell probabilities as well as size of the region considered. (Banik et al., 2002) applied Markov chains to analyze the probabilities of transitions from a ‘dry week’ to a ‘non dry’ or a ‘dry week’ aimed at developing an index of drought proneness for a given region.(Steinemann, 2003) adopted six classes of severity, from wet to dry conditions, relative to the PDSI and the SPI, and used the homogeneous Markov chain formulation to characterize the steady-state probabilities, and the probabilities for drought class transition and for duration in a class. The results obtained allowed the author to propose triggers for activating drought preparedness plans at the basin scale. Other Markov chains applications were recently published but concern dry spells, not early warning.

3.3. Role of Markov random field in remote sensing

Markov Random Fields (MRF) are commonly used probabilistic models for image analysis (Li, 2001).The basic idea of MRF is to model the contextual correlation. The continuous enhancement of the satellite remote sensor's characteristics (e.g., improved spatial and spectral resolutions and reduced revisit time) has increased the importance of remote sensing in real-world applications such as mapping, agriculture, forestry, oil and mineral extraction, fishing, environmental monitoring, and disaster prevention and monitoring. The information provided by individual sensors is incomplete, inconsistent, or imprecise. Additional sources may provide complementary data, and the merging of the multi-source data can create a more consistent interpretation of the scene. Indeed, focusing on classification-based image analysis, it has been shown in the literature that the integration of the context into a classification scheme can significantly improve the results in terms of accuracy and reliability. The first work on MRF based statistical methodology for image analysis application was employed by Geman and Geman in the year 1984 (Li, 2001).

(Solberg et al., 1996) proposed MRF based model for classification of multi-source satellite imagery. Their model exploits spatial class dependencies between neighbouring pixels in an image, and temporal class dependencies between different images of the same scene. They also compare the performance of MRF based model with simpler reference fusion model. On the basis of the well-founded theoretical basis of MRF for classification tasks and the encouraging experimental results in study, they proposed MRF model as a useful tool for classification of multisource satellite imagery.

The MRF models had been widely used in image change detection. In order to increase the accuracy of the final change detection map, (Bruzzone and Prieto, 2000) integrated spatial contextual information in their unsupervised change detection scheme through an MRF model that exploits interpixel class dependences to model the prior probabilities of change and no-change classes, by including the temporal aspect of the data, the model was found to be suitable for detection of class changes between the acquisition dates of different images. (Bruzzone and Prieto, 2002) also developed an MRF-based adaptive semi parametric technique that makes use of the Reduced parzen estimate (RPE) and the E–M algorithm to estimate in an unsupervised way the changes that may occur in a temporal sequence of images.(Kasetkasem and Varshney, 2002), addressed the problem of image change detection based on MRF models. They modelled MRF by using noise lese images obtained from the actual scene and change images in order to search for an optimal image of changes by applying the maximum a posterior probability (MAP) decision criterion and the Simulated Annealing energy minimization procedure.

(Melgani and Serpico, 2003) proposed a "mutual" MRF approach that integrate spatio-temporal contextual information into the classification scheme considerably improves the accuracy values over those obtained by using a conventional non-contextual classification method. They carried out a bidirectional exchange of the temporal information between the defined single-time MRF models of consecutive images. They also proposed a simple and fast method based on the concept of "minimum perturbation" and implemented it with the pseudo inverse technique for automatic determination of the MRF model parameters which yielded significant results that make it an attractive alternative to the usual trial-and-error search procedure. The author has

stated the usefulness of MRF in many image-processing areas such as image restoration, image and texture synthesis, segmentation, classification and surface reconstruction.

(Solberg et al., 2004) presented a framework for flexible nonlinear contextual image classification. The framework integrates classical and recent models for image classification, ranging from a multivariate Gaussian classifier, to MLP neural nets, classification trees and recent regression models based on general additive models, and combines them with a Markov random field for spatial context. The effect of using the different nonlinear discriminant functions was compared with the effect of using an MRF model for spatial context. The use of an MRF model resulted in larger improvements in classification accuracy than different nonlinear discriminant functions, but the combination of them can give more large improvements even.

(Kasetkasem et al., 2005) employed MRF for land cover mapping at sub pixel level. They proposed method that was able to generate super-resolution land cover maps from remote sensing data. In the proposed MRF model based approach, the intensity values of pixels in a particular spatial structure (i.e., neighbourhood) are allowed to have higher probability (i.e., weight) than others. Remote sensing images at two markedly different spatial resolutions, IKONOS MSS image at 4 m spatial resolution and Landsat ETM+ image at 30 m spatial resolution, was used to illustrate the effectiveness of the proposed MRF model based approach for super-resolution land cover mapping. There was significant increase in the accuracy of land cover maps at fine spatial resolution over that obtained from linear optimization approach.

(Tso and Olsen, 2005), implemented MRF based method using both contextual information and multiscale fuzzy line process for classifying remotely sensed imagery. The proposed classification approach uses panchromatic image for extracting multiscale line features by means of wavelet transform techniques. The resulted multiscale line features was merged through a fuzzy fusion process and then incorporated into the MRF model accompanied with multispectral imagery to perform contextual classification so as to restrict the over-smooth classification patterns and reduce the bias commonly contributed by boundary pixels. The model parameter was estimated based on the probability histogram analysis to boundary pixels, and the algorithm called maximum a posterior margin (MPM) was applied to search the solution. The results show that the proposed method, based on the MRF model with the multiscale fuzzy line process, successfully generates the patch-wise classification patterns, and simultaneously improved in classification accuracy by adding contextual and edge information into the classification pool.

(Liu et al., 2006) proposed a spatial-temporal classification algorithm for forest disease monitoring that explicitly classify individual images using spectral, spatial and temporal information. They concluded that MRF can be used as efficient probabilistic models for the analysis of spatial and temporal contextual information.

Thus it can be conclude that these reviews highlight the numerous efforts made till date with developing relationship between various satellite and meteorological derived indices to point out a specific type of drought caused either by rainfall deficiency, or less vegetation vigour or low agricultural production. In the present study, both meteorological indices (SPI) and satellite based drought indices (SVI) have been used to assess the drought. Drought has spatio-temporal

behaviour. So it is important to study the temporal as well as spatial nature of drought. The previous study provides a basis for analytical investigation of spatio-temporal pattern of droughts. Therefore, this research adopt Three-dimensional Markov random field to model spatio-temporal pattern of drought.

4. Materials and Methods

This chapter gives a brief overview of the data used and the methodology adopted to work out the proposed research.

4.1. Data acquisition

Data has been acquired mainly from two sources, firstly NDVI derived from satellite sources and secondly rainfall obtained from ground rainfall stations.

4.1.1. Satellite data acquired / NOAA-AVHRR NDVI data

The NOAA-AVHRR – NDVI composite which is provided by Global Inventory Modeling and Mapping studies (GIMMS) was downloaded from the University of Maryland Global Land Cover Facility Data Distribution centre.

4.1.1.1. Spatial Characteristics

Spatial Coverage:
The coverage is global for all land areas except Greenland and Antarctica.
Spatial Resolution:
The composite data has a spatial resolution of 8 km in Albers Equal Area Conic projection using the Clarke 1866 ellipsoid. The continental file of Eurasia (EA) was downloaded and the study area was extracted.

4.1.1.2. Temporal Characteristics:

Temporal Coverage:
The dataset has a temporal coverage from July 1982 to December 2003.
Temporal Resolution:
Monthly GIMMS dataset is a 15-day time step composite data. The 15a composite is the maximum value composite from the first 15 days of the month, and the second 15b is from days 16 through the end of the month. Using 15a and 15b, the maximum value composite was calculated in order to get the monthly datasets.

GIMMS NDVI has been corrected for:

- Residual sensor degradation and sensor intercalibration differences;
- Distortions caused by persistent cloud cover globally;
- Solar zenith angle and viewing angle effects due to satellite drift;
- Volcanic aerosols;

- Missing data in the northern hemisphere during winter using interpolation due to high solar zenith angles;

- Low signal to noise ratios due to sub-pixel cloud contamination and water vapour.

Table 4-1 Data Descriptions of NOAA-AVHRR- NDVI Composite Source: GLCF

Parameter/ Variable name	Parameter/ variable Description	Data range	Units of measurement	Data source
GIMMS	GIMMS* Normalized Difference Vegetation Index calculated From AVHRR channel 1 and 2 digital count data.	Theoretical range between -1 and 1; values around 0 for bare soil (low or no Vegetation) values of 0.7 or larger for dense vegetation. Water = -0.1 No Data = -0.05	Unit-less	AVHRR

4.1.2. Meteorological data

Monthly rainfall datasets were acquired for the period of 22 years ranging from 1982-2003 for the Gujarat state. Monthly rainfall for 169 rain stations which is shown in Figure 4-1 has been used to derive Standardized Precipitation Index (SPI). The data has been collected from Bhaskaracharya Institute of Satellite and Geoinformation (BISAG), Gandhinagar and Agro-Meteorological Department, Anand Agriculture University, Anand. The number of rainfall stations for a period between 1982 to1989 was 168, from 1990 to 1997 the number of these stations increased to 174 and in the year 2000-2003 the number of rainfall stations was 218 . Therefore to maintain consistency in data, rainfall data for 164 rain stations for which rainfall data was available for a period of 22 years was considered in carrying out the required analysis.

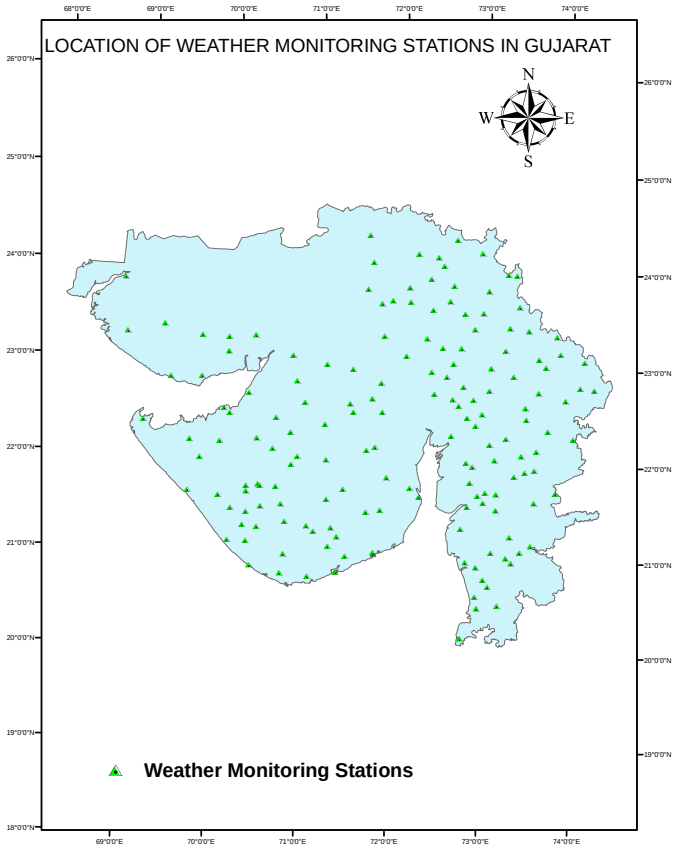

Figure 4-1 Gujarat map showing Weather monitoring Stations

4.2. Methods

4.2.1. Research Methodology

The methodology adopted in this research is based on the formulation of the research question, literature study and concept built during the course period. The methodology developed for this study is shown in Figure 4-2.

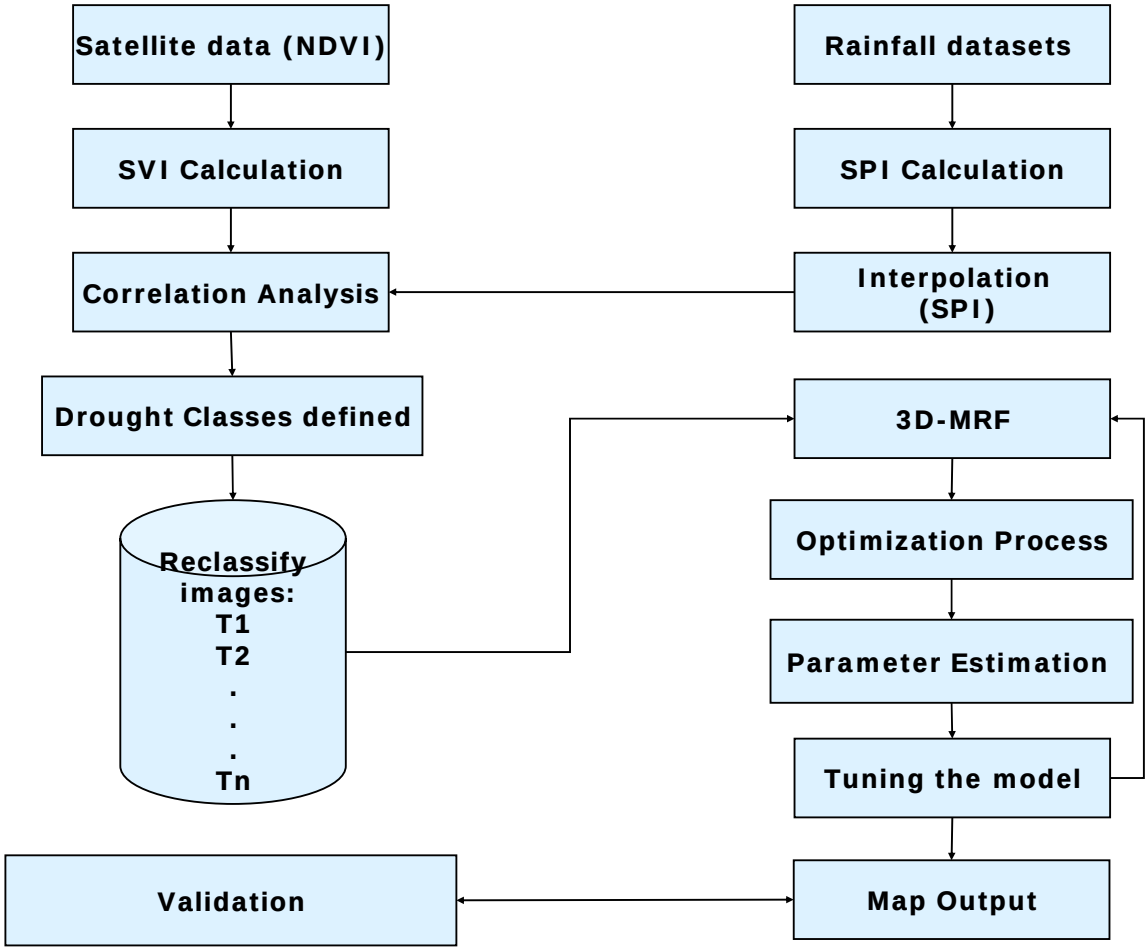

Figure 4-2 Overall approach of the study

4.2.2. Pre-processing of Satellite data:

All the twenty two years of NDVI-AVHRR datasets were imported to ENVI 4.1 and were rescaled to get the NDVI values ranging from -1 to +1 by using the Band math function. Compositing process was carried out to select the pixels with high NDVI values to get a cloud free image.

4.2.3. Computation of SVI:

NOAA-AVHRR- NDVI data sets from 1982 to 2003 was used to calculate the Standardized Vegetation Index. The SVI is based on calculation of a Z-score for each AVHRR pixel location. The Z score is a deviation from the mean in units of the standard deviation, calculated from the NDVI values for each pixel location for each month for each year, during the n-years as

$$Z_{ijk} = \frac{\left(NDVI_{ijk} - NDVI_{ij}\right)}{\sigma_{ij}}$$

Where

$NDVI_{ijk}$ = highest NDVI value for pixel *i* during month *j* for year *k*,
$NDVI_{ij}$ = mean NDVI for pixel *i* during month *j* over *n* years
σ_{ij} = standard deviation of pixel *i* during month *j* over *n* years.

After the calculation of Z- score for each pixel, the probability of that score was determined as

$$SVI = P(Z_{ijk})$$

This per pixel probability is expressed as the Standardized Vegetation Index (SVI), is an estimate of the "probability of occurrence" of the present vegetation condition which was calculated using the program that was written in IDL 6.1.

4.2.4. Computation of SPI:

Monthly Rainfall data for 164 rainfall stations were arranged according to format defined by (National Drought Mitigation Center, 2006) to have input to SPI program. SPI was computed for each station on time scale 1, 2, 3, 6, 9 and 12.

4.2.5. Interpolation of Standardized precipitation index:

As mentioned earlier SPI was developed to quantify precipitation deficit at different time scales SPI was interpolated for five months i.e. June, July, August, September and October for the time period from 1982 to 2003. Point map of all weather stations in Gujarat was prepared from the lat/long file in order to add each month to the map and interpolate it accordingly.

Initially SPI values had been interpolated using Inverse Distance Weighted (IDW) technique taking grid size of 8km. IDW interpolation explicitly implements the assumption that objects that are close to one another are more alike than those that are farther apart (ArcGIS 9.0) Interpolation has been performed in ArcGIS 9.0. But in the present work interpolation by IDW did not gave good results. Kriging has provided optimal areal estimates in any given situation and is applicable both for drought and flood (Kassa, 1999). Therefore the ordinary kriging was performed for the interpolation of SPI in R Software. Kriging is a statistical interpolation method that is optimal in the sense that it makes best use of what can be inferred about the spatial structure in the surface to be interpolated from an analysis of the control point data. The predictions are weighted linear combinations of the available data. The interpolated maps are thus been reclassified into different drought severity classes.

4.2.6. Three-dimensional Markov Random field Model Framework:

4.2.6.1. Concept of Context:

Meteorological and agricultural drought occurrences along time and space take place randomly and therefore their scientific quantifications are possible by the probabilistic methods. Herein Drought characteristics of any phenomenon are assumed to have spatial and temporal stationarity with underlying independent generating mechanism and can be modelled by suitable technique. In interpretation of drought condition, context is very important. Contextual information is ultimately necessary in the interpretation of visual information. It is one kind of spatial relationship and has drawn our particular interest for remotely sensed imagery interpretation shown in this study. Contextual information, or so-called context for simplicity, may be defined as how the probability of presence of one object (or objects) is affected by its

(their) neighbours. It may be derived from spectral, spatial or even temporal attributes. In this study, the spatial and temporal dimension has been focused upon. Spatial context shows the spatial relationship between spatially neighbouring pixels within the predefined neighbourhood system. The temporal dimension is defined between the multiple images of the same area. A scene is understood in the spatial and visual context of the objects in it; the objects are recognized in the context of object features.

Using concept of context, pixel in the image are not treated in isolation, but are considered to have relationship with their neighbours. Thus the relationship between pixel of interest and its neighbours are treated as being statistically dependent. A nearest neighbourhood dependence of pixels on an image lattice is obtained by going beyond the assumption of statistical independence. Information on the nearest neighbourhood is used to calculate conditional probabilities.

Generally, in drought Modeling through remote sensing, a pixel labelled as class of moderate drought is likely to be surrounded by the same class of pixels unless it is located on the boundary. Incorporating contextual information into Drought Modeling can be done in different ways. One simple method of adopting context is to use majority voting within a prescribed window. In such a method, the central pixel will be changed to the class that occurs most frequently in the window. There are more elegant ways of Modeling such contextual behaviour.

A class of contextual model known as Markov random field (MRF) can be useful for Modeling context in a more precise way .It is a probabilistic model defined by the local conditional probabilities. Markov random field (MRF) theory provides a convenient and consistent way for Modeling spatial–temporal contextual information in terms of conditional prior probabilities. MRF is used to construct a priori probability in Bayesian sense so as to accomplish the Maximum a Posteriori (MAP) estimate during the Modeling process. Maximum a posterior (MAP) probability is one of the most popular criteria for optimality and widely applied for MRF Modeling (Li, 2001).

In order to maintained consistency in thesis, standardization of symbol was done.

Table 4-2 Legend of notation for Markov random field model

Symbol	Explanation
M, N	Image Dimension (M is no. of row and N is no. of column)
K	Number of drought classes
P(wk)	Prior Probability for class wk
c (i, t)	Class value of site i at time t, class is defined as drought class based on SVI
d (i, t)	Class value of site i at time t, class is defined as drought class based on SPI
U_{sp}	Spatial prior energy function
U_{td}	Temporal Dependence energy Function
c_t	Set of class labels for the scene at time t
c (Ns (i, t))	Class vector of Spatial neighbourhood of site i at time t

Z	Normalizing constant also called partition function
Model Parameters	
β_{sp}	Parameter to control the spatial energy
β_{td}	Parameter to control the temporal dependence energy

4.2.6.2. Initialization of the image configuration:

Suppose the M * N image which consist of MN pixels or sites. The scene consists of K true drought classes (which is defined on the basis of SVI /SPI), w1, w2 ….wk, with prior probabilities P (w1)…, P (wk). The class label of pixel i is denoted by c(i, t) or d(i, t). Let Xs denote the set of pixels for the whole scene that is,

Xs = {Xs (i, j); $1 \leq i \leq M$, $1 \leq j \leq N$}, and

C = {c (i, t)| d (i, t); $1 \leq i \leq M$, $1 \leq j \leq N$}.

The corresponding set of labels for the whole scene: c (i, t) or d (i, t) is an element of {w1, w2… wk}.

For initialization of the image configuration, class temporal prior probability was calculated for each class label at each pixel position considering number of temporal observations. For each pixel location that class label was chosen which maximizes the class temporal prior probability. The expected output from this step was used to initialize the optimization process.

4.2.6.3. Optimization process:

The second phase was based on an optimization algorithm which can iteratively update each pixels with new class labels in such a way the global energy associated with it is minimum .Since, MRF model has a flexible framework for combinations of the contextual information from neighbouring pixels and the information from the distribution of the data, the image was modelled by using MRF model. Two energy functions were defined to introduce contextual information and class temporal prior probability concept was introduced for non-contextual information. These energies are combined to yield a global energy. Then pixel labelling was accomplished by minimizing the global posterior energy by using suitable algorithm. In order to formulate the problem using MRF, it is necessary to introduce the concept of spatio-temporal neighbourhood system adopted in the next subsection.

Neighbourhood system used:

Consider a Set {S} that denotes the set of sites defined over an image. The sites in *S* are related to one another via a neighbourhood system. A neighborhood system for *S* is defined as:

$$N = \{N_i \mid \forall i \in S\} \qquad \textbf{Equation 4-1}$$

Where N_i is the of sites neighboring i. The neighborhood system has the following properties:-

1) A pixel can not be a neighbour to itself.
2) The neighbouring relationship is mutual.

In the first order neighbourhood system, also called the 4-neighborhood system, every site has 4-neighbors which share a side with the given site. In Second order neighbourhood system, every site has 8-neighbors which share a side with the given site.

Although it is possible to use various spatial neighbourhood systems, Second order neighbourhood is considered to be enough in some of the previous MRF studies (Hailu Kassaye, 2006; Kasetkasem et al., 2005 ; Kasetkasem and Varshney, 2002). Hence, a second order neighbourhood system or window size 3 was considered in the present research. The following Figure 4-3 shows the spatial-temporal neighbourhood system used in this study.

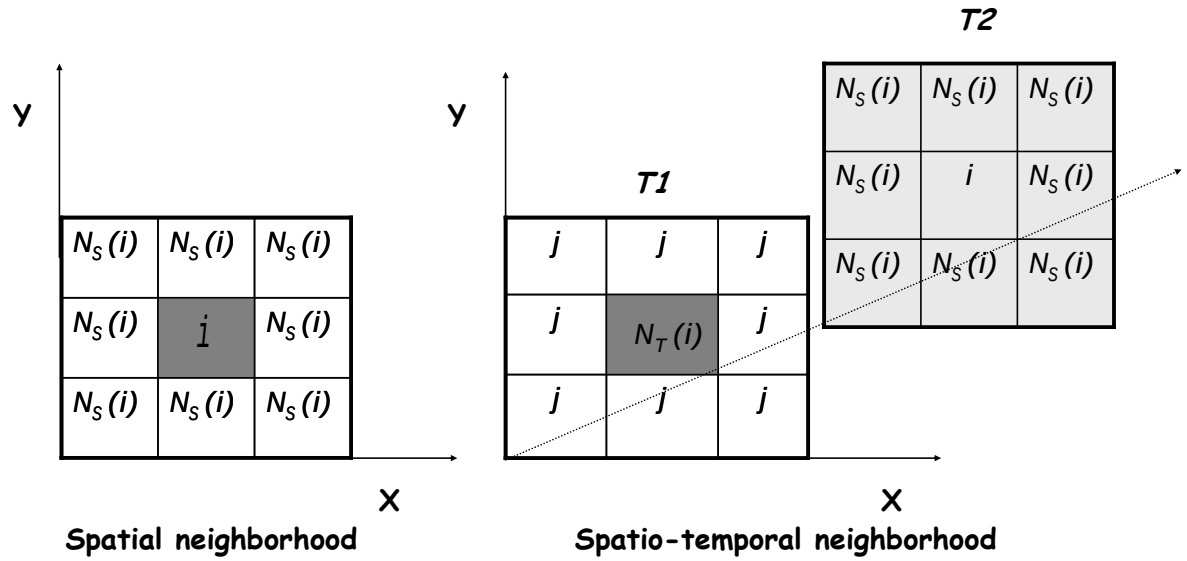

Figure 4-3 MRF neighbourhood systems

(Note: spatial neighbourhood (Left); spatio-temporal neighbourhood. Axes X, Y are the spatial coordinates of sites. Axis T is the temporal index of the sites (Right).)

Markov Random Fields and Gibbs random fields

Let a set of random variables $d = \{d_1, d_2 \ldots d_m\}$ be defined on the set S containing m number of sites in which each random variables y_i $(1 \leq i \leq m)$ takes a label from label set *L*. The family d is called a random field. The set S is equivalent to an image containing *m* sites; *d* is a set of sites DN values; and the label set L depends upon the application. The label set L is equivalent to a set of the user-defined information classes, e.g. L = {Severe drought, Moderate drought etc}. A random field d, with respect to neighbourhood system, is a Markov random field if its probability density function satisfies the following properties.

Positivity: P(d) > 0, this first property, that of positivity, can usually be satisfied and the joint probability P(d) can be uniquely determined by local conditional probabilities.
Markovianity: P (d r | d s-r) = P (d r | d Nr) shows that labelling of a pixel of interest only dependent on its neighbouring pixels.
Homogeneity: P (d r | d Nr) is same for all sites r. it specifies the conditional probability for the label of a pixel, given the labels of the neighbouring pixels, regardless of the relative location of the pixel.

Where "S-r" is the set difference (i.e. all pixels in the set S excluding r, d_{s-r} denotes the set of labels at the sites in "S – r", N_r denotes the neighbours to pixel r.

Besides these above three properties, MRF may also incorporate other properties, such as isotropy which describes the direction-independence i.e. the neighbouring sites surrounding a site r have the same contributing effect to the labelling of site r.

Any random variable d is said to be a Gibbs random field (GRF) on set S with respect to neighbourhood N if and if its configurations obey a Gibbs distribution in the following form:

$$P(d) = \frac{1}{Z} \times \exp\left[\frac{-U(d)}{T}\right] \qquad \textbf{Equation 4-2}$$

P (d) measures the probability of the occurrence of particular configuration or "pattern", d.
U (d) is called and energy function
T is a constant termed temperature which should be assumed to be 1 unless otherwise stated.
Z is normalizing constant also called partition function and can be expressed as

$$Z = \sum \exp\left[\frac{-U(d)}{T}\right] \qquad \textbf{Equation 4-3}$$

From above it is clear that maximizing P (d) is equivalent to minimizing the energy function U (d).

Formulation of the objective function:

Spatial energy function:
The spatial energy was defined as favoring small changes in the drought class and penalizing the large ones. The spatial energy function encourages neighbouring pixels to be classified with the same labels and thus impose a spatial smoothness effect. Both the spatial and temporal energy functions require the definition of a neighbourhood system. In our case, a second-order neighbourhood system is adopted. Specifically, the spatial energy function involved in MRF is specified as:

$$U_{sp}\left(c(i,t), c\left(N_s(i,t)\right)\right) = \beta_{sp} \sum_{j \in N_s(i)} \left(c(i,t) - c(j,t)\right)\text{^}2 \qquad \textbf{Equation 4-4}$$

Temporal dependence energy function:
Temporal neighbors contribute to the energy function in a probabilistic sense which is specified by transitional probability concept. In our spatial-temporal approach, the temporal relation is modeled by a transition probability matrix which defines the probability of one pixel belonging to one drought class at a time T1 given that it belongs to another class at time T2. Specifically the temporal dependence energy function in MRF model is formulated as

$$U_{td}\left(d(i,t_1),c(i,t_2)\right) = -\beta_{td} \cdot \ln\left(P(c(i,t_2) \mid d(i,t_1)\right) \quad \textbf{Equation 4-5}$$

Construction of global posterior energy:

Bayes statistics is a theory of fundamental importance in estimation and decision making. When the context is introduced as prior information and modeled by means of MRF, Bayesian framework can be adopted to construct the global energy and labeling is carried out by minimizing this global posterior energy, since energy and probability are inversely proportional, one can say that the lower the energy the higher is the probability of labeling. Information on the nearest neighborhood is used to calculate the conditional probabilities. In this study we applied the assumption of MRF being isotropic and homogeneous for the neighboring pixels in the same neighborhood order. The global posterior energy is defined as:

$$U_{Global} = U_{sp} + U_{td} \quad \textbf{Equation 4-6}$$

The optimal class label $\hat{w}_j$ can be found by minimizing the global posterior energy, to get the optimal solution maximum a posterior (MAP) was adopted as:

$$\hat{w}_j = \underset{w_j \in c(i,t)}{Min}\left(U^i_{Global}\left(w_j\right)\right) \quad \textbf{Equation 4-7}$$

Simulated annealing

After the construction of the global posterior energy, the next step was to perform pixel labeling by minimizing the global posterior energy. One would like to obtain a pixel labeling that is reasonable to the data and the prior model. A popular criterion is to find the labeling that maximizes the posterior distribution (MAP). Three algorithms, namely Iterated conditional modes (ICM), Maximum a Posterior Marginals (MPM) and Simulated Annealing (SA) can be used to obtain global minimum energy. These algorithms are iterative in nature.

Simulated annealing algorithm was adopted to find the MAP solution. Simulated annealing is a type of stochastic algorithm for combinatorial optimization. The concept of simulated annealing is equivalent to the introduction of the noise in to the system to shake the search process away from the local minimum. The idea is similar to a process in metallurgy in which a small region of a metal structure is heated until it is pliable enough to be reconstructed in to the desired shape. The metal is then cooled very slowly to make sure that it is given enough time to respond. Changes in temperature must be very small until the metal is hardened. The whole process is controlled by initial temperature and updating schedule. Initially the process is started at high temperature; this means that a high temperature can increase the probability of a pixel being replaced by new class label even though the new class label has high energy. The temperature is decreased according to predefined cooling schedule. In this study we adopted following equations for the cooling schedule.

$$T = \frac{T_0}{\log\left(1 + beta(K+1)\right)} \quad \textbf{Equation 4-8}$$

Where T_0 is initial temperature
beta is a constant which represents how much the temperature would decrease for every iteration. It is called as descent constant or other wise called as "Rate of fall".
K denotes the number of iteration.

The pixel updating was performed according to the energy difference between old class label and new class label. If the energy of the old class label was higher than the new class label, than pixel was replaced by the new class label. The iteration was repeated for each temperature update value.

Parameter estimation:
MRF models make use of parameters that weigh the influence of information sources on the decision process. This can be viewed as a way of expressing the degree of confidence (reliability) in each information source. In practice, the MRF parameters permit one to "tune up" the MRF model in order to get optimal solution. The determination of the MRF parameters is not a trivial problem. The larger the number of information sources, the larger the number of MRF parameters and the more difficult the parameter estimation. In this study, minimum perturbation method was used to estimate the MRF parameters. Let us consider image consists of M sites i.e. S_i (i = 1, … M).The first step of the method consists in computing the total energy associated with each pixel i.e. class label w_j (j = 1, 2,…, 5) associated with that pixel, under the assumption that all the information sources have the same reliability weights. In other words, the following energy is computed for each pixel associated class label.

$$U^i_{Global}(w_j) = U^i_{sp}(w_j) + U^i_{td}(w_j) \qquad \textbf{Equation 4-9}$$

The optimal class $\hat{w}_i$ for the site S_i is one that satisfies

$$U^i_{Global}\left(\hat{w}_i\right) = \underset{w_j \in c(i,t)}{Min}\left(U^i_{Global}\left(w_j\right)\right) \qquad \textbf{Equation 4-10}$$

The "minimum energy perturbation" is defined as the smallest additional amount of energy required to classify the Pixel class label correctly (Melgani and Serpico, 2003).

$$\Delta U^i = \left[U^i_{Global}\left(\hat{w}_j\right) - U^i_{Global}\left(w_j\right)\right] \times (1+\delta) \qquad \textbf{Equation 4-11}$$

Where w_i stands for the true class of the pixel i and δ is an arbitrary small positive constant. Then after the computation of the minimal energy perturbation for each pixel class label, the second step of method consists in estimating the values of parameters that satisfy the following systems of equations:

$$\begin{bmatrix} U_{sp}^{1}\left(w_t^1\right) & U_{td}^{1}\left(w_t^1\right) \\ U_{sp}^{2}\left(w_t^2\right) & U_{td}^{2}\left(w_t^2\right) \\ \cdot & \cdot \\ \cdot & \cdot \\ U_{sp}^{m}\left(w_t^m\right) & U_{td}^{m}\left(w_t^m\right) \end{bmatrix} \cdot \begin{bmatrix} \beta_{sp} \\ \beta_{td} \end{bmatrix} = \begin{bmatrix} T^1 \\ T^2 \\ \cdot \\ \cdot \\ T^m \end{bmatrix}$$ **Equation 4-12**

Where T^i (i = 1… *m*) given by

$$T^i = U_t^i\left(w_t^i\right) + \Delta U^i$$ **Equation 4-13**

To find an approximate solution for such a system characterized by a number of equations larger than the number of unknowns is to adopt the minimization of the sum-of-squared error as a criterion and to apply the technique based on the pseudo-inverse matrix for its optimization. By rewriting the system of equations in terms of matrices:

$$\bar{U} \cdot \bar{\beta} = \bar{T}$$ **Equation 4-14**

To estimate the optimal MRF parameter vector β^* is given by the following expression based on the pseudo-inverse of the matrix U:

$$\beta^* = \left(U^{tr}U\right)^{-1}U^{tr}\,\bar{T}$$ **Equation 4-15**

Where *tr* is transpose of the matrix.

The method is applied in the context of the initialization step of the simulated annealing algorithm.

5. Results and Conclusion:

5.1. Mean vegetation and rainfall patterns

On average most of the rainfall (400 – 1500 mm) received in Gujarat state occurs between June and October, with maxima in July. Approximately 90% of the annual rainfall falls between June and October, so averaging rainfall and NDVI data for these months fairly represents the main growing season for the region. Figure 5-1 illustrates the mean evolution of rainfall and NDVI, respectively. Overall mean total rainfall shows increasing trend from north western to south eastern region. This rainfall pattern corresponds well with the NDVI. The north-west and central and south-west part of region comparatively less rainfall and vegetation signal represented by compared to eastern and south-eastern part of the region

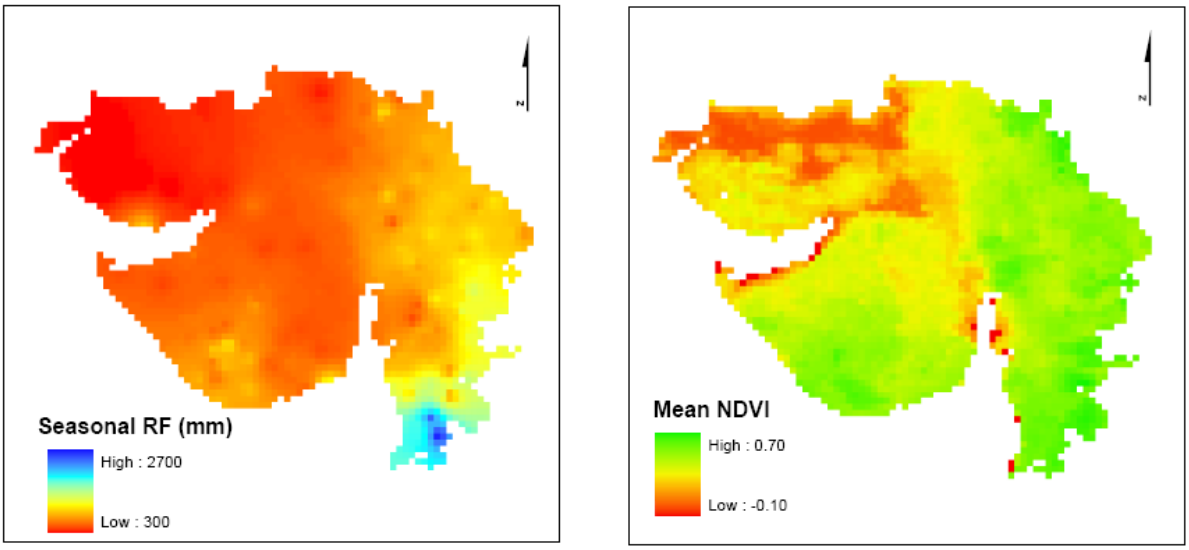

Figure 5-1 Spatial Patterns of Mean Seasonal Rainfall (Left) and NDVI (Right) in Gujarat.

5.2. Interpolation of SPI

The rainfall data are point measurements, the satellite values are average over pixel-sized areas. A geostatistical technique of interpolation i.e. Ordinary kriging was performed with grid size of 8 Km and seasonal maps for 22 years were prepared. Variograms help to reveal the spatial dependence of the rainfall points i.e. it reveals the maximum distance where one point influences another, for different stations. The spatial continuity of the data was examined on the basis of the variogram analysis. Variogram for different months were made to get the sill, range, partial sill and nugget. Variogram for the July month is shown in Figure 5-2.

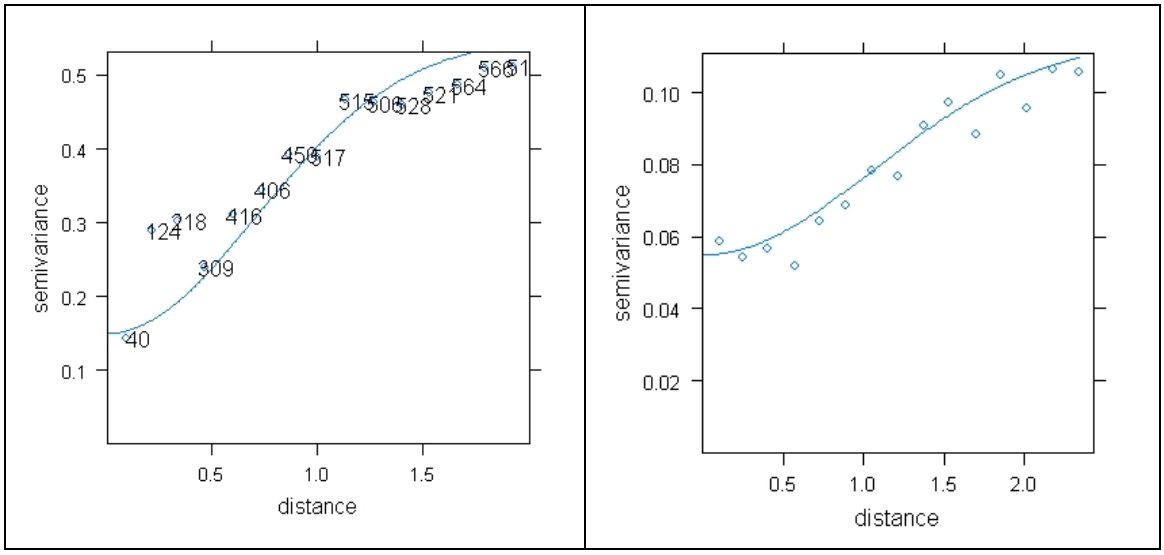

Figure 5-2 Modelled Variogram for SPI- JULY -1987 (Left) and SPI- JULY-1988 (Right)

Table 5-1 Details of the Variogram

	SPI – JULY -1987	**SPI – JULY -1988**
PARTIAL SILL	0.30	0.045
RANGE	1.25	1.66
NUGGET	0.15	0.055
LAG SIZE	8000	8000
MODEL	GAUSSIAN	GAUSSIAN

5.3. Significance of SPI as drought monitoring tool

SPI is used for quantification of precipitation deficit at different time scales. Since SPI gives the indication of drought characteristics like onset, severity and spatial extent. Therefore it can be used as drought monitoring tool.

5.3.1. Selection of drought sensitive station:

For the identification of the drought sensitive stations, SPI data from 1982 to 2003 for the month of July was used. The onset of monsoon starts in the month of July, so the SPI values for 164 meteorological stations were analyzed in order to identify drought sensitive stations. Out of 164 meteorological stations three stations were found to be most sensitive stations which is shown in Figure 5-3.

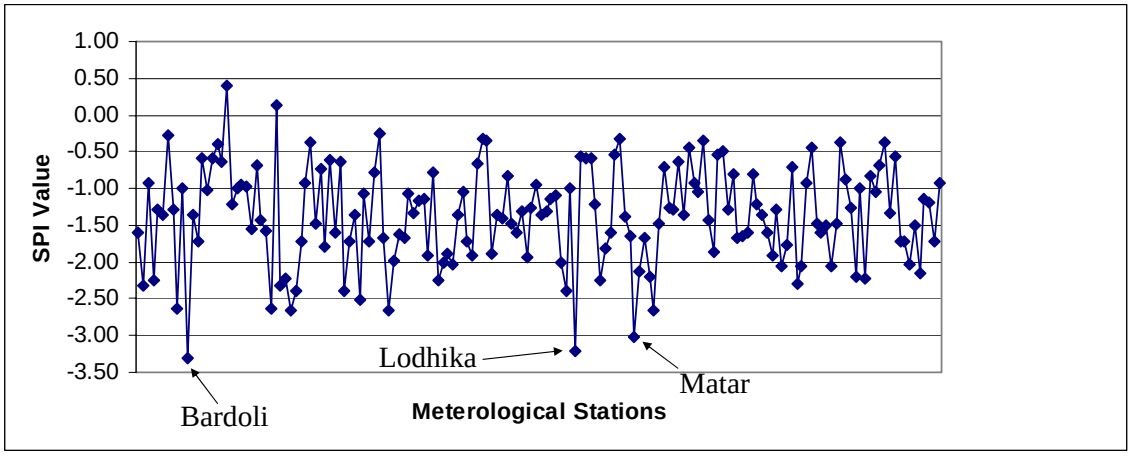

Figure 5-3 Selection of drought sensitive stations using SPI

5.3.2. Selection of drought year

For the selection of the drought year from 1982 to 2003, SPI was used. The year corresponding to lowest SPI within the time series was taken and considered as drought year. It can be clearly seen in the Figure 5-4, that lowest SPI value was observed in the year 1987. So year 1987 was considered as drought year and similarly, year 1988 was chosen as a wet year.

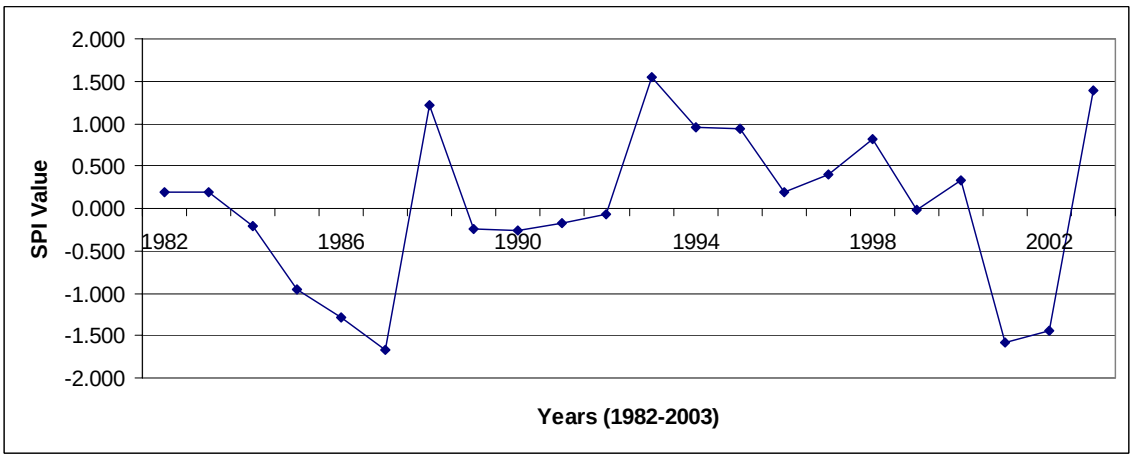

Figure 5-4 Selection of drought sensitive year using SPI value Recorded at Mehsana

5.3.3. SPI and drought

SPI during selected drought years 1987 and normal years of 1988 have been presented to show the spatial pattern of SPI during these years. From Figure 5-5, it can be depicted that year 1987 was a drought year whereas year 1988 was a normal one. There is clear indication that during the drought years of 1987, SPI values are low for the North-eastern, western, central and south-western Gujarat, which indicates that there has been low rainfall in these areas. SPI in 1987 indicated that, 1987 was an extreme severe drought year, where SPI was found to be below (-3.18). However during the normal years of 1988 SPI reached up to a value of 2.8, which states that 1988 was wet year.

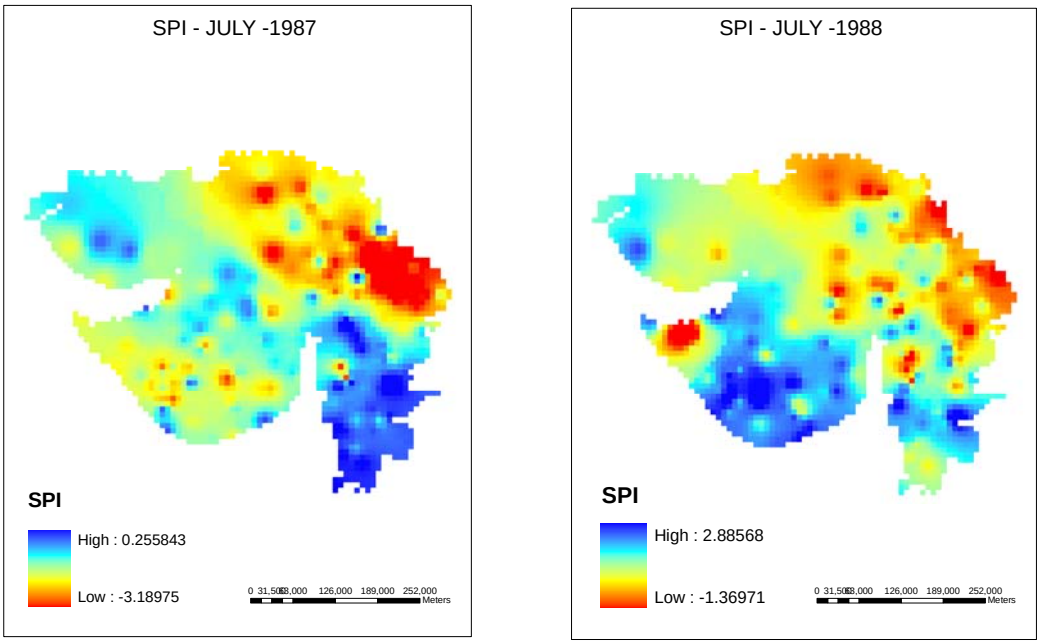

Figure 5-5 1-month SPI for selected drought and wet years

5.3.4. SPI as indicator of onset of drought

Onset of drought can be detected with the help of SPI. Using SPI values, all the interpolated SPI maps were classified into five drought classes. Classified drought map of the year 1987 for the month June, July, august and September is shown in the Figure 5-6

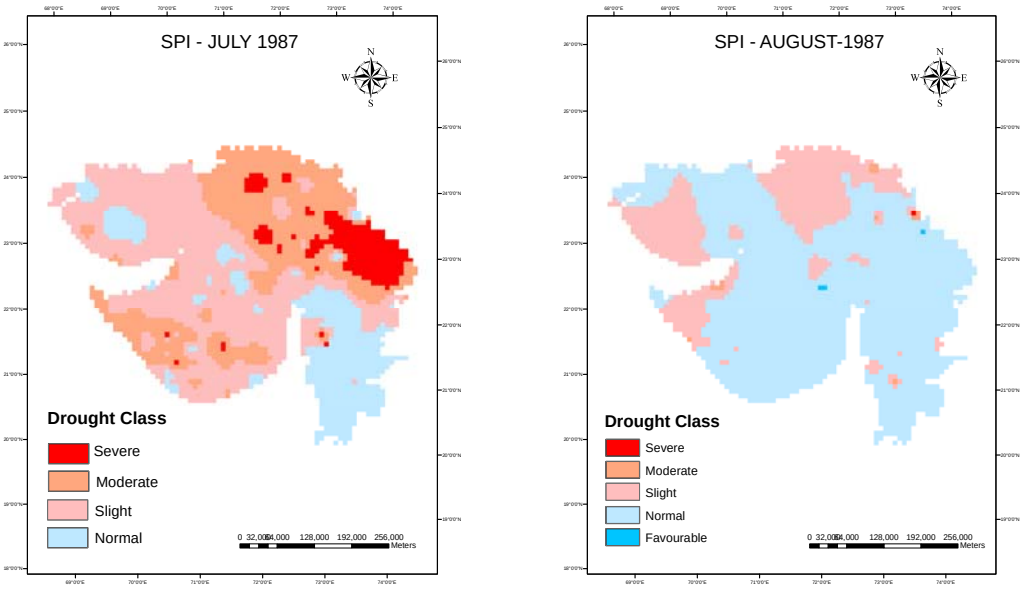

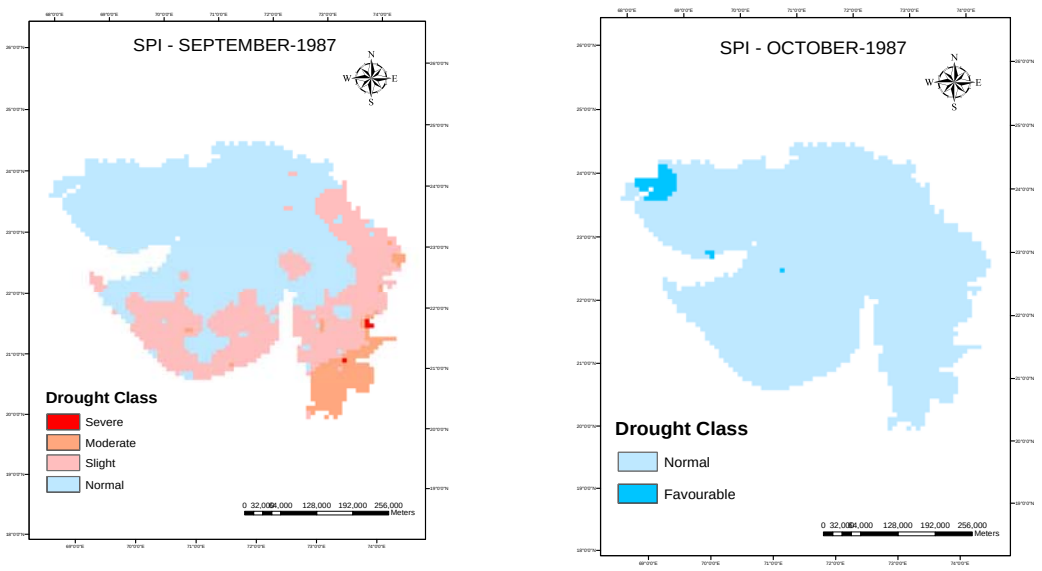

Figure 5-6 Interpolated SPI map for the month July, August, September and October 1987

5.4. Standardized Vegetation Index

The Standard Vegetation Index (SVI) is based on the fact that vegetation conditions are closely linked to weather conditions in the atmosphere closest to the ground. It shows us the effects of climate on vegetation health. From Figure 5-7 it can be depicted that SPI has highlighted Normal condition over the whole Gujarat State. At the same moment of time SVI has highlighted the Vegetation health was not good. So it becomes advantage of SVI over SPI in pre-identification of drought occurrence.

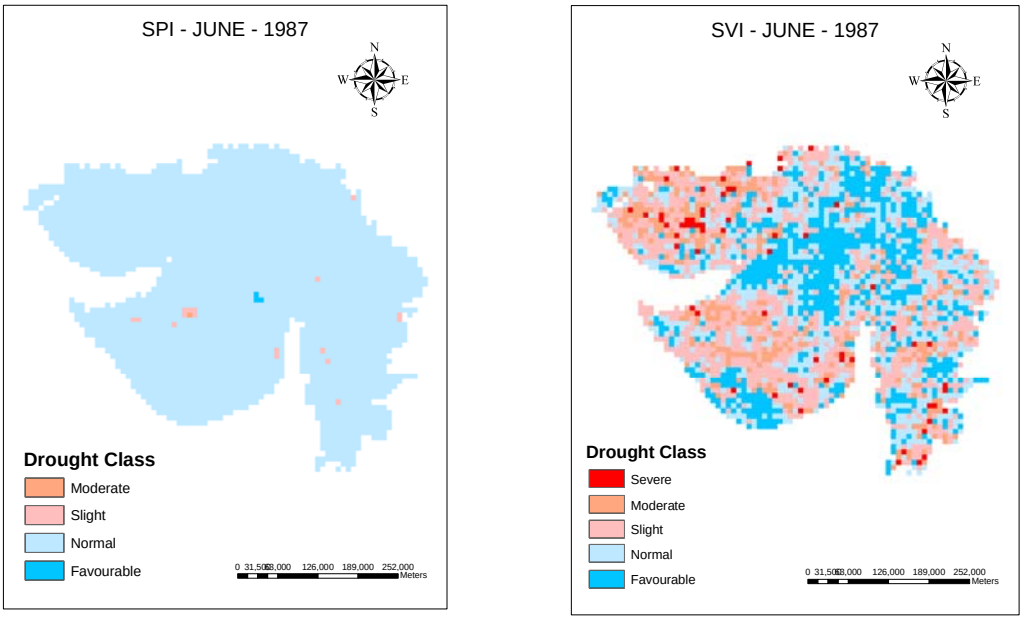

Figure 5-7 SPI (Left) and SVI (Right) for June 1987.

5.5. Covariation of SPI and SVI time series

The relationship between vegetation and moisture availability was clarified by analyzing the co variation of SVI and SPI time series with the scatter plots and correlation analysis. SVI time series data for each of the 164 rain stations was extracted from the 22 years SVI time series images. Correlation coefficient between SPI and SVI was calculated. Generally there is a time lag between precipitation events and response of vegetation to such events. The time interval between a precipitation event and the time when precipitated water might reach a plant root and affect plant growth can vary from 1 to 12 weeks depending on vegetation type (Ji and Peters, 2003) . In order to account for this interval and assess the real maximum correlation between SVI and SPI the SVI/rainfall correlation coefficients were calculated for time lags of 0,1 and 2 months. Out of three lag-time, the correlation coefficient for time lag of 1 month was found to be higher than others one. (Rundquist et al., 2000)found the lag time of vegetation response to precipitation was approximately 1 month. Mathematically the relation can be written as following:

$$SVI_t \approx f\left(SPI_{t-1}\right) \qquad \textbf{Equation 5-1}$$

Where *t* denotes month.

Representative points for agro-climatic zones of Gujarat were selected for analysis. Correlation analysis was carried out for the month of June to October between SPI and SVI from the period 1982-2003 to analyze the temporal pattern of SPI and SVI and to see variation in vegetation according to rainfall.

Table 5-2 Correlation analysis between SPI and SVI for time lag of 1-month

STATION NAME	SPI(JUNE) –SVI (JULY)	SPI(JULY) – SVI (AUGUST)	SPI(AUGUST) – SVI (SEPTEMBER)	SPI (SEPTEMBER) – SVI (OCTOBER)
NAKHTRANA	0.06	0.56	0.317	0.57
HIMATNAGAR	0.49	0.144	0.46	0.72
JHAGADIA	0.47	-0.08	0.14	0.12
LAKHTAR	0.40	0.05	0.29	0.14
DHORAJI	0.24	0.03	0.39	0.37
JAMNAGAR	0.45	0.19	0.48	0.26
RAJKOT	0.19	0.28	0.52	0.29

It can be noted from Table 5-2, that significant correlation exists between SPI and SVI in different months. When comparing the correlation coefficients with the vegetation phonological cycle, it is clear that vegetation response to moisture availability varies significantly between months.

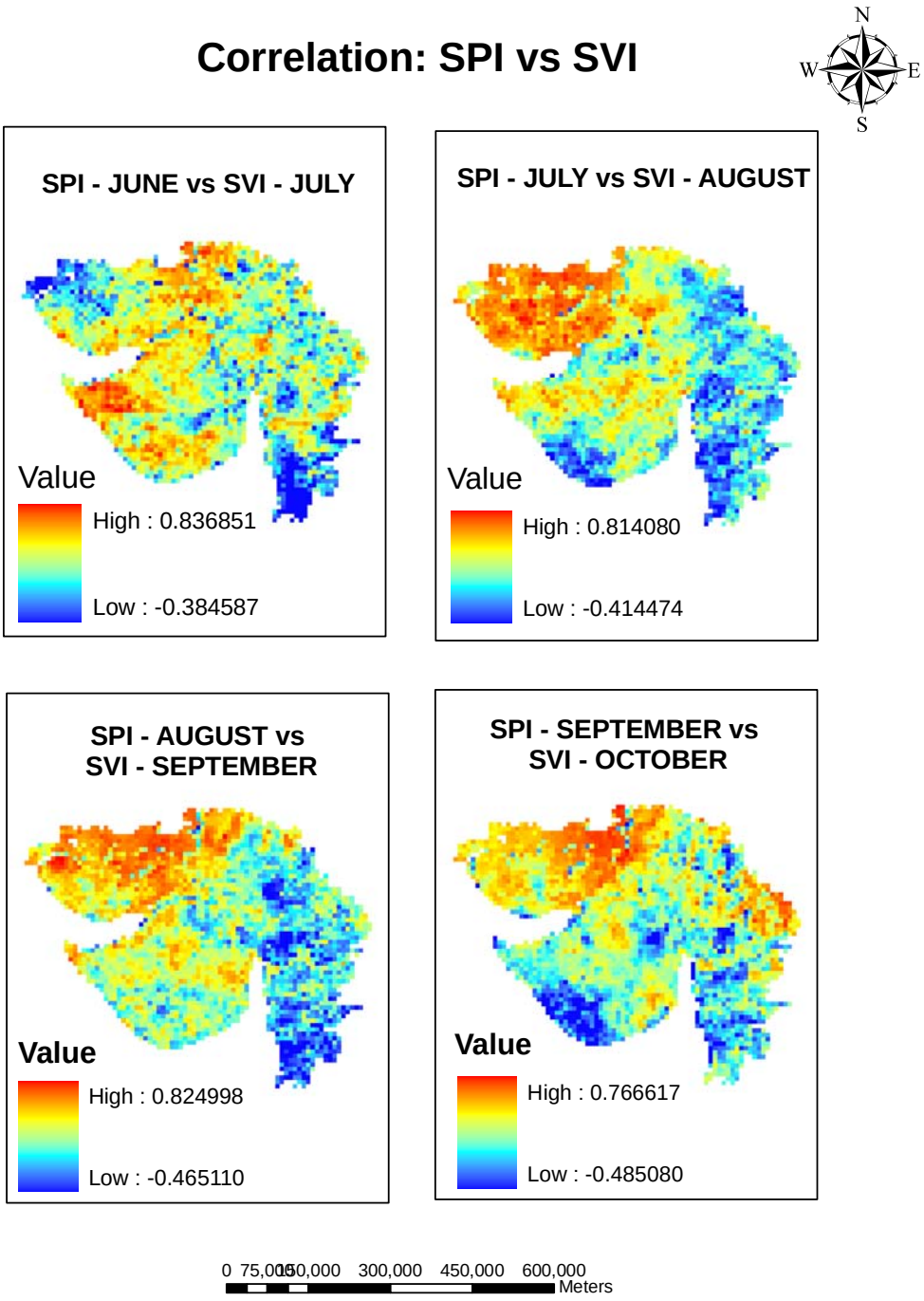

Figure 5-8 Spatial correlation analysis between SPI and SVI considering Lag affect.

Spatial Correlation analysis was carried out for month of June to October between SPI and SVI from the period 1982-2003 considering lag effect which is shown in Figure 5-8. Correlation between SPI and SVI on lag effect was found to be positive in north and northern-western part of Gujarat for all months. Reason behind positive correlation could be because of rain fed crops. The lowest correlation values appear in south Gujarat, which is high rainfall area (1000 mm – 2500 mm) where as high correlation (> 0.4) is vigilant in arid and semi-arid areas of north

Gujarat and central part of Kathiawar peninsula. These are the areas where annual rainfall is between 400- 700 mm. maximum correlation values are obtained in this region because precipitation event serves as primary source of water for plant growth.

5.5.1. Goodness-of-fit of the SPI – SVI correlation:

The relationship between the SVI and 1-month SPI was tested using R^2 from the simple linear regression model. An attempt was made to search for the best fit curve. From the Figure 5-9 and Figure 5-10 it can be depicted and in general it was found that polynomial of higher order gives better $R^{2.}$

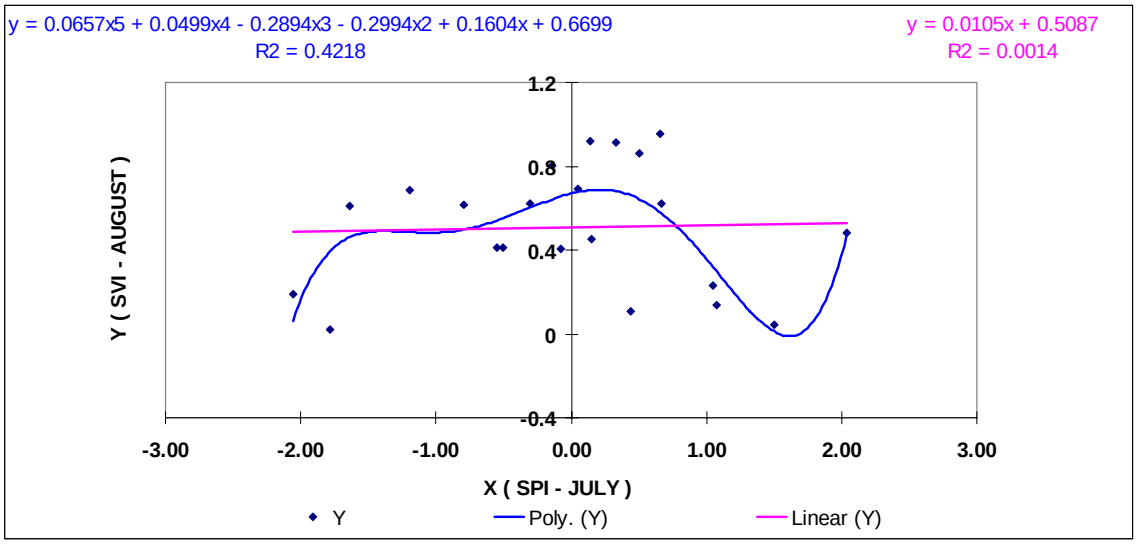

Figure 5-9 Best fit curve for the rainfall station Dhoraji

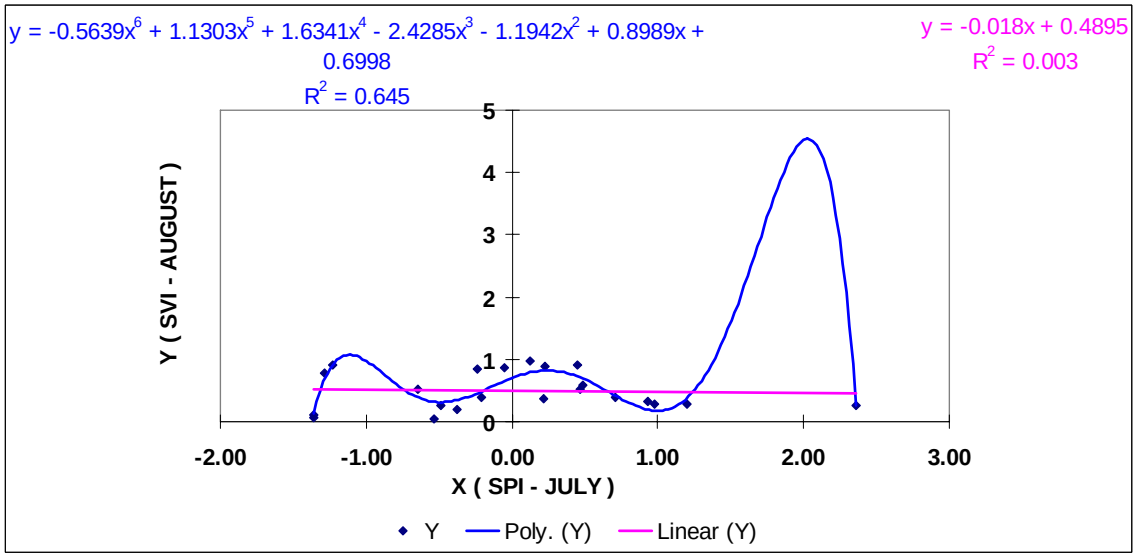

Figure 5-10 Best fit curve for the rainfall station Lakhtar

5.5.2. Generalized Classification of drought classes

The generalized classification of the drought classes was done based on the observed relationship between SPI and SVI. All the SPI and SVI images were reclassified accordingly which is shown in Table 5-3

Table 5-3 Drought Severity Classification (modified)

SPI VALUES	DROUGHT CLASS
-2 to less	Severe drought
-1.5 to -1.99	Moderate drought
-1.0 to -1.49	Slight drought
-0.99 to 0.99	Normal
1.0 to 2.0+	Favourable

(Source: http://drought.unl.edu/monitor/spi)

For the Standardized Vegetation index (SVI) images, five drought classes have been defined in terms of data descriptor which is shown in Table 5-4

Table 5-4 Classification of SVI in terms of data descriptor.

SVI VALUES	DROUGHT CLASS
0 - 0.10	Severe drought
0.10 - 0.25	Moderate drought
0.25 - 0.5	Slight drought
0.5 - 0.75	Normal
0.75 – 1	Favourable

In order to implement the MRF model and for simplicity the drought classes were reclassified. So images consist of only numbers i.e. 1, 2, 3, 4 and 5. Each number corresponds to different drought class.

Table 5-5 Representation of drought classes.

SPI AND SVI VALUES\RECLASSIFICATION	
Severe drought	1
Moderate drought	2
Slight drought	3
Normal	4
Favourable	5

5.6. Identification of drought pattern at next time moment using Three-dimensional Markov random field

Several attempts were made to understand and illustrate the capability of three-dimensional Markov random field model for identification of drought pattern at next time moment using spatio-temporal information.

Trial model framework: There are three basic issues to make model framework:

- How to represent the problem in mathematical form?
- How to formulate an objective function for the Model?
- How to optimize the objective function?

These three issues are related to each other. In the first place, the scheme of representation influences the formulation of objective function and on other hand; the formulation of objective function affects the search. Initially, we tried to make the model framework considering three moment of time. To represent the problem, the objective functions were defined in the form of energy.
For example, to identify the drought pattern say august 2003 in terms of SVI. The three moment of time were T1 as SPI image June 2003, T2 as SVI image July 2003 and T3 as what we have to identify the drought at third moment of time, the spatial energy function works on at T3 image, the temporal dependence energy function works between T1 image and T2 image, as this function uses the concept of transitional probability. The temporal dependence energy function was later found to be incompletely defined; it must include T2 image and T3 image for the calculation. Ignoring it was equivalent to throwing away important source of information. Therefore modification of expression was done for the temporal dependence energy function. Since the first model was inconsistent because it did not consider two moment of time, the whole model was changed accordingly.

A code was written in IDL 6.1, to develop the three-dimensional Markov random field model.

Model layout:
To identify the pattern of drought at next time, initially the class temporal prior probability was calculated by considering the temporal images for each pixel values. That class label was chosen which maximize the class temporal probability. It was done in order to get an image that can be used as an initial image for the optimization process. The spatial energy function encourages neighboring pixels to be classified with the same class labels and thus imposes a spatial smoothness effect on the final prediction. The temporal dependence energy function was calculated in terms of transitional probability, thus updating the prediction with important source of information, then at each step updating of class label was done in such a way that global posterior energy is minimized. So global posterior energy i.e. spatial energy function and temporal dependence energy which involves the pixel of interest was computed for all possible updates of the class labels and new class label was chosen that correspond to lowest energy value. The replacement of old class label with new one was done and then the model proceeds to next pixel. If the optimal class label was the same as before the update, then it was not considered as a successful update. Otherwise it was considered as a successful update. During

optimization process, different experiments were performed to obtain the optimal parameters value using different training datasets. Several attempts were made to find good set of MRF parameters which is in next subsection.

Optimization Process:

Experiment 1:

An experiment was performed to obtain the optimal parameters value. The initial temperature was set to 100. To estimate the parameter value, training dataset was used. An image of SPI, June 1987 was used. For the initialization purpose the image from 1982 to 1986 of SVI July was used to calculate the temporal class probability. During this process the temperature is lowered slowly until it reaches to a freezing state. The optimization process converges to minimum energy after 32 iterations. The optimal parameters value obtained are:

$\beta_{sp} = 0.0162306$

$\beta_{td} = 0.377119$

Using the above parameters value, the estimation of SVI 1987, July, August, September and October was done. SVI July 1987 prediction matches with reference data which is shown in Figure 5-11.

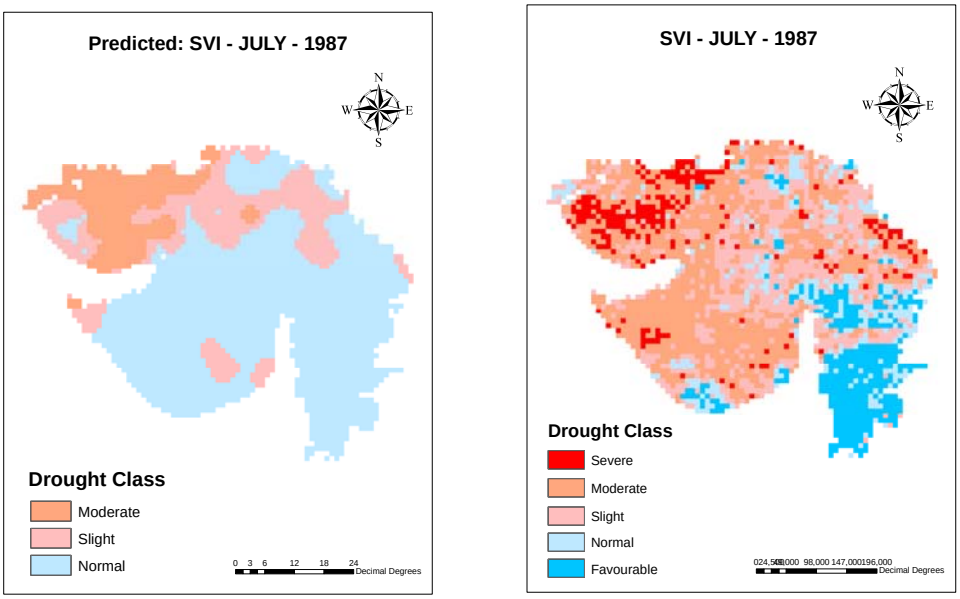

Figure 5-11: Predicted image of SVI July 1987 (Left) and Reference data- SVI July 1987 (Right) for Experiment 1.

Experiment 2:

An experiment was performed to obtain the optimal parameters value. The initial temperature was set to 100. To estimate the parameter value, training dataset was used. An image of SPI, August 2002 was used. For the initialization purpose the image from 1982 to 1986 of SVI September was used to calculate the temporal class probability. During this process the

temperature is lowered slowly until it reaches to a freezing state. The optimization process converges to minimum energy after 66 iterations. The optimal parameters value obtained are:

$\beta_{sp} = 0.00048$
$\beta_{td} = 0.128913$
Using the above parameters value, the estimation of SVI 1987, July, August, September and October was done. The predicted SVI July 1987 and the corresponding reference data is shown in Figure 5-12.

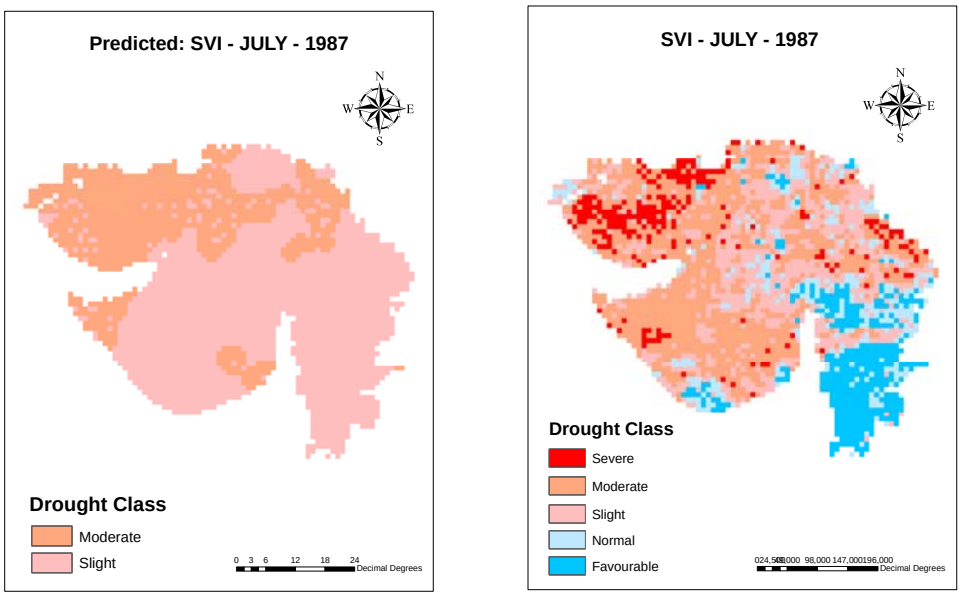

Figure 5-12: Predicted image of SVI July 1987 (Left) and Reference data- SVI July 1987 (Right) for Experiment 2.

Experiment 3:

An experiment was performed to obtain the optimal parameters value. The initial temperature was set to 100. To estimate the parameter value, training dataset was used. An image of SPI, June 2002 was used. For the initialization purpose the image from 1982 to 2001 of SVI July was used to calculate the temporal class probability. During this process the temperature is lowered slowly until it reaches to a freezing state. The optimization process converges to minimum energy after 66 iterations. The optimal parameters value obtained are:

$\beta_{sp} = 0.0000325211$
$\beta_{td} = 0.0155076$
Using the above parameters value, the estimation of SVI 2002, July, August, September and October was done which is shown in Figure 5-13.

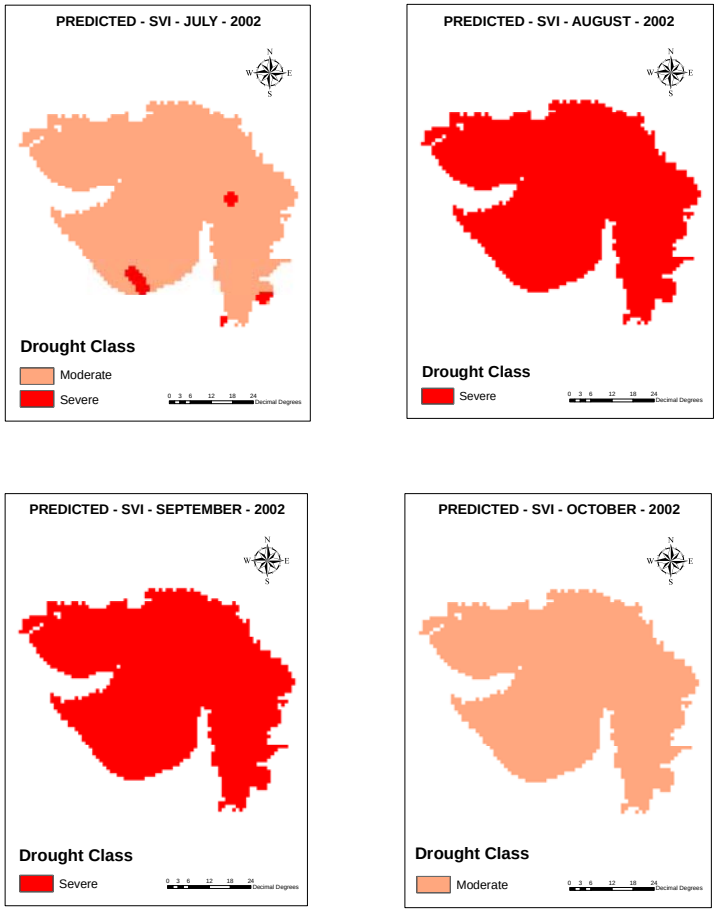

Figure 5-13: Predicted image of SVI July, August, September and October 2002 respectively for Experiment 3

Experiment 4:

An experiment was performed to obtain the optimal parameters value. The initial temperature was set to 100. To estimate the parameter value, training dataset was used. An image of SPI, July 2002 was used. For the initialization purpose the image from 1982 to 2001 of SVI August was used to calculate the temporal class probability. During this process the temperature is lowered slowly until it reaches to a freezing state. The optimization process converges to minimum energy after 13 iterations. The optimal parameters value obtained are:

$\beta_{sp} = 0.00552183$

$\beta_{td} = 0.729557$

Using the above parameters value, the estimation of SVI 2002, July, August, September and October was done which is shown in Figure 5-14.

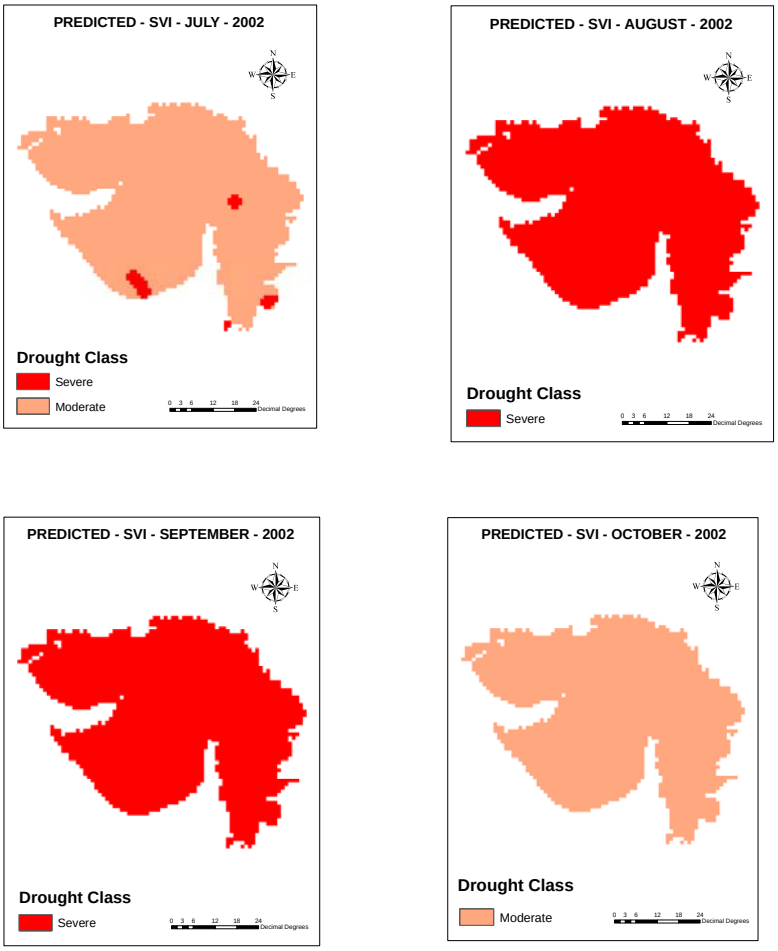

Figure 5-14: Predicted image of SVI July, August, September and October 2002 respectively for Experiment 4

Experiment 5:

An experiment was performed to obtain the optimal parameters value. The initial temperature was set to 100. To estimate the parameter value, training dataset was used. An image of SPI, August 2002 was used. For the initialization purpose the image from 1982 to 2001 of SVI September was used to calculate the temporal class probability. During this process the temperature is lowered slowly until it reaches to a freezing state. The optimization process converges to minimum energy after 14 iterations. The optimal parameters value obtained are:

$\beta_{sp} = 0.000738915$

$\beta_{td} = 0.645072$

Using the above parameters value, the estimation of SVI 2002, July, August, September and October was done which is shown in Figure 5-15.

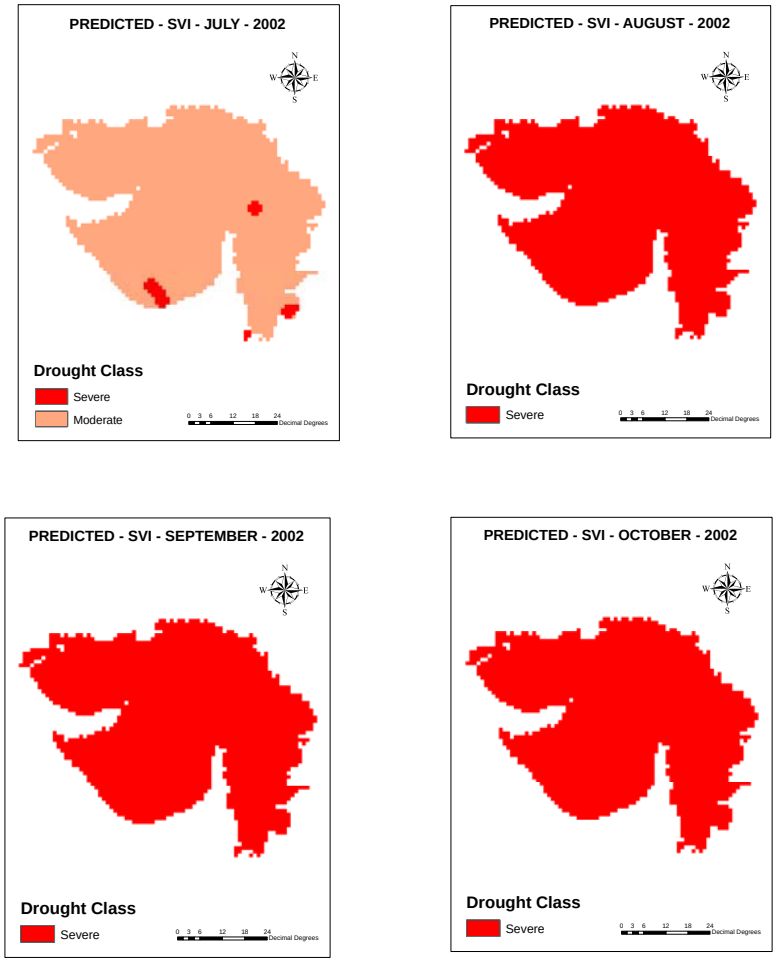

Figure 5-15 Predicted image of SVI July, August, September and October 2002 respectively for Experiment 5.

Experiment 6:

An experiment was performed to obtain the optimal parameters value. The initial temperature was set to 100. To estimate the parameter value, training dataset was used. An image of SPI, September 2002 was used. For the initialization purpose the image from 1982 to 2001 of SVI October was used to calculate the temporal class probability. During this process the temperature is lowered slowly until it reaches to a freezing state. The optimization process converges to minimum energy after 21 iterations. The optimal parameters value obtained using the mentioned scenario is:

$\beta_{sp} = 0.0962934$

$\beta_{td} = 0.181716$

Using the above parameters value, the estimation of SVI 2002, July, August, September and October was done which is shown in Figure 5-16.

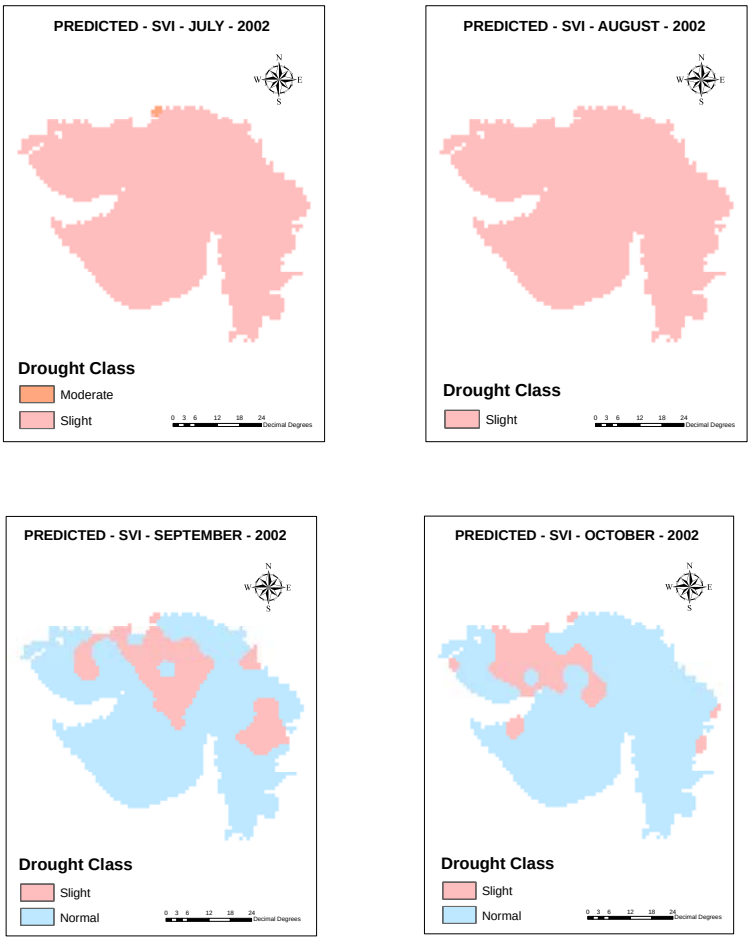

Figure 5-16: Predicted image of SVI July, August, September and October 2002 respectively for Experiment 6.

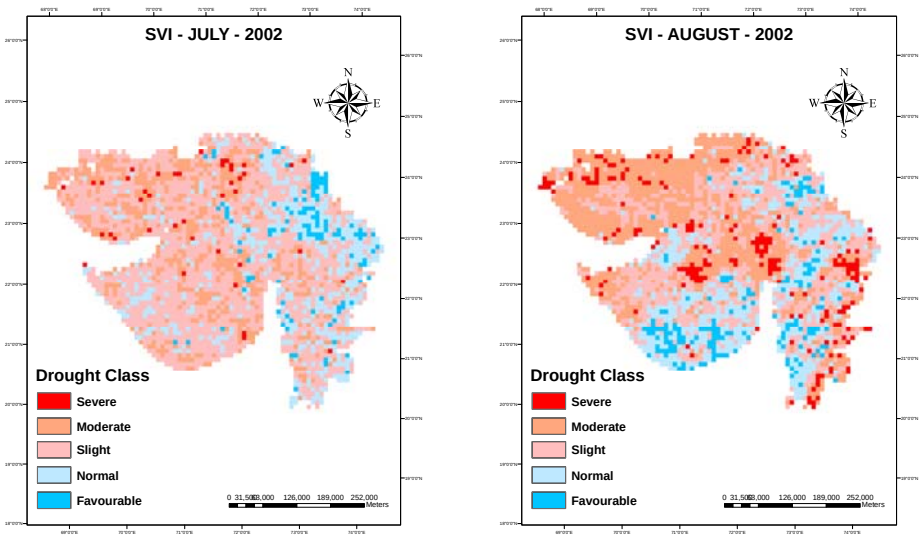

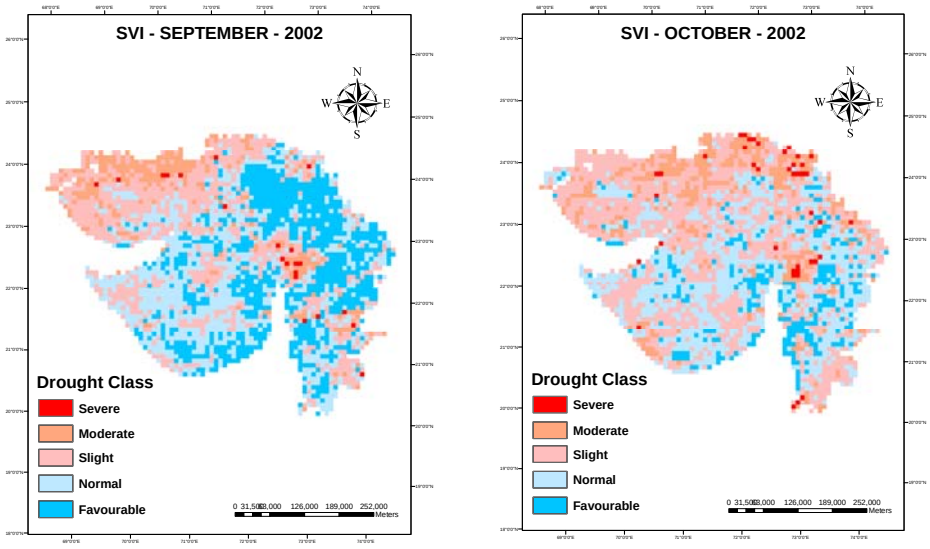

Figure 5-17 Reference image of SVI July, August, September and October 2002 respectively for Experiment 3, 4, 5, 6 and7.

The comparison of the above experimental results was carried out with reference data. It is concluded that there is no unique optimal parameter value that can optimize the prediction quality of all transitions of all possible data. The reason for not getting the required result depends on how well the relationship is defined between SPI and SVI. The relationship between the SPI and SVI has affected the model output because the model was implemented according to the assumption that the SVI reflects the state of vegetation at the given moment and SPI influences the state of vegetation in the future, this effect was modeled in terms of energy function in the MRF. If the output of a model is not what was expected, there are two possible reasons:

- The formulation of the objective function was not appropriate one for Modeling the complex phenomenon like drought.
- The output was a low quality local minimum

The most important aspects of the energy function are its form, involved parameters and the corresponding assumptions made during the Modeling. The form and parameters together define the energy function which in turn defines the minimal solution. The form and parameters depends on the assumption about the expected solution and the observed data. Since the parameters are part of the definition of the energy function, the solution is not completely defined if the parameters are not specified even if the functional form is known. The above mentioned reason may deviate the solution from the expected.

Selection of factors that affect the drought Modeling is also a crucial component. The factors such as soil moisture, temperature, evaporation, relative humidity, evapo-transpiration, wind speed affect the drought Modeling. One of possible reason for not getting the expected output was the above mentioned constraints or factors which affect the drought prediction was not embedded in to the energy function. The energy functions defined in this study was done using only first order approach. This may be one of the possible reasons that affect the output.

In general one can conclude that, the ability to extract drought in automated fashion will contribute to further spatio-temporal analysis of drought Modeling. This work using a spatio-temporal explicit algorithm in drought monitoring context has broader applicability across different applications using temporal remote sensing imagery. The overall methodology presented in this paper provides a general framework on the use of spatio-temporal information from NDVI time series data. As such the new method is not limited to the specific data used in this work. However, the spatio-temporal information might vary its value in different applications with different spatial resolution and temporal frequency of images.

6. Conclusions and Recommendation

The main objective of the study was to build a tool for identification of drought pattern using three-dimensional Markov random field.

In order to address the objectives three research questions were posed during this study. Several experiments were carried in order to provide answers for the raised questions.

The first research question examine that how to quantify the drought classes using NDVI and rainfall in terms of data descriptor. It was concluded from the study that the temporal variations of SVI are closely linked with precipitation and there exists a significant correlation for time lag of 1 month between SVI and 1-month SPI.

It was found that rainfall has positive relation with SVI and also correlation of rainfall/SVI was found to be strong in water limiting areas, which states that these areas are more prone to drought. Based on the relationship between the SVI and SPI, generalized classification of drought class was done and five drought classes were defined. Finally the quantification of drought class in terms of data descriptor was presented.

It was found that using SPI one can compare rainfall of two areas with different rainfall characteristics. Thus SPI can be used for the indication of the drought characteristics at the spatial level.

NDVI time series was subjected to scale to Standardized vegetation index in order to monitor the drought. By identifying the relationship between SPI and SVI, It was concluded that at some location were SPI was unable to show the drought area, SVI get advantage over SPI. Thus integration and analysis of drought identified areas from SPI and SVI, help in correctly identifying the region affected by drought

The second research question was how to incorporate the NDVI and rainfall in MRF model. The model incorporates the relationship between the SPI and SVI i.e. SVI reflects the state of vegetation at the given moment and SPI influences the state of vegetation in the future, this effect was modeled in terms of energy function in the MRF.

The third research question tells about the proper parameter setting in the MRF model and the method adopted for the parameter estimation. Proper parameter setting can lead to a successful result. So it was necessary to search the optimal parameters values. According to the experimental results, it is concluded that there is no unique optimal parameter value which can optimize the prediction quality of all transitions of all possible data. The reason for not getting the expected output depends on the assumptions that were made during the Modeling. The model was implemented according to the assumption that lag time of vegetation response to precipitation was approximately 1 month. From the previous studies, it was found that

vegetation response to precipitation was 4-8 weeks depending on the vegetation cover types. Sine the lag time is not known exactly, the output of the model was affected. The validation of model was done with mentioned reference data. The prediction of SVI July 1987 using parameter values 0.0162306, 0.377119 were found optimal for that drought year. The choice of the energy functions has also affected the model output. For the parameter estimation, the simple and fast method "the minimum perturbation energy" was used to get the values.

A tool to model spatio-temporal pattern of drought using Three-dimensional Markov random field was developed. The model in the present state worked well with assumption taken in present study. Since drought Modeling is affected by many parameters, the model can be improved by incorporating more parameters (soil moisture, temperature, evaporation, relative humidity, evapo-transpiration, wind speed) in form of well defined energy function.

Recommendation

The developed MRF program used in this study can be tried out using 3-month SPI and SVI or NDVI based on the fact that the 3-month SPI has best correlation with NDVI.

As three-dimensional Markov random field is a new technique, therefore a lot of research is to be carried out to enhance this method.

7. References

National Drought Mitigation Center,2006. What is drought. National Drought Mitigation Center, USA.

Anyamba, A. and Tucker, C.J., 2005. Analysis of Sahelian vegetation dynamics using NOAA-AVHRR NDVI data from 1981-2003. Journal of Arid Environments, 63(3): 596-614.

Banik, P., Mandal, A. and Rahman, M.S., 2002. Markov chain analysis of weekly rainfall data in determining drought-proneness. Discrete Dynamics in Nature and Society, 7(4): 231-239.

Bavadam, L., 2001. Dealing with drought Frontline, pp. 09-22.

Brown, F.J., Reed, C.B., Hayes, J.M., Wilhite, A.D. and Hubbard, K., 2002. A Prototype drought monitoring system integration climate and satellite data Pecora 15/Land Satellite Information IV/ISPRS Commission I/FIEOS 2002 Conference Proceedings

Bruzzone, L. and Prieto, D., 2000 Automatic analysis of the difference image for unsupervised change detection Ieee Transactions on Geoscience and Remote Sensing 38(3): 1171-1182

Bruzzone, L. and Prieto, D., 2002. An adaptive semiparametric and context-based approach to unsupervised change detection in multitemporal remote-sensing images IEEE Transactions on Image Processing 11(4): 452-466

Cazacioc, L. and Cipu, E.C., 2004. Evaluation of the transition probabilities for daily precipitation time series using a Markov chain model, 3-rd International Colloquium ”Mathematics in Engineering and Numerical Physics”. Balkan Society of Geometers, Geometry Balkan Press 2005, Bucharest, Romania.

Edwards, Daniel, C., McKee and Thomas, B., 1997. Characteristics of 20th Century Drought in the United States at Multiple Time Scales. Climatology Report No. 97-2, Department of Atmospheric Science, Colorado State University, Fort Collins, CO 80523-1371.

Gore, P.G. and Ponkshe, A.S., 2004. Drought in Gujarat Districts and State as key indicators to all India drought. Journal of Agrometerology, 6(1): 47-54.

Gupta, R., 2000. Water governance in Gujarat state, India International Journal of Water Resources Development, 20(2): 131-147.

Hailu Kassaye, R., 2006. Suitability of Markov random field based method for super resolution land cover mapping, ITC, Enschede, 77 p. pp.

Hayes and Michael, J., 2006. Drought Indices National Drought Mitigation Center USA.

Hayes, M., Svoboda, M., Wilhite, D. and Vanyarkho, O., 1999 Monitoring the 1996 drought using the standardized precipitation index Bulletin of the American Meterological Society 80(3): 429-438

Ji, L. and Peters, A.J., 2003. Assessing vegetation response to drought in the northern Great Plains using vegetation and drought indices. Remote Sensing of Environment, 87(1): 85-98.

Jurgen, V.V., Alain, A.V., Isbelle, B., Stefan, N. and Francesca, S., 1998. Drought Monitoring from Space Using Empirical Indices and Physical Indicators, International Symposium on 'Satellite-Based Observation"-A Tool for study of the Mediterranean basin',Tunis,Tunisia. Joint Research Centre of European Commission.

Kasetkasem, T., Arora, M. and Varshney, P., 2005 Super-resolution land cover mapping using a Markov random field based approach Remote Sensing of Environment 96(3-4): 302-314

Kasetkasem, T. and Varshney, P., 2002 An image change detection algorithm based on Markov random field models Ieee Transactions on Geoscience and Remote Sensing, 40(8): 1815-1823

Kassa, A., 1999. Drought Risk Monitoring for the Sudan using NDVI 1982-1993, University College London, 39 pp.

Kogan, F.N., 1990. Remote-Sensing of Weather Impacts on Vegetation in Nonhomogeneous Areas. International Journal of Remote Sensing, 11(8): 1405-1419.

Li, J., Lewis, J., Rowland, J., Tappan, G. and Tieszen, L.L., 2004. Evaluation of land performance in Senegal using multi-temporal NDVI and rainfall series. Journal of Arid Environments, 59(3): 463-480.

Li, S.Z., 2001. Markov Random Field Modeling in Image Analysis Springer-Verlag Telos, 323 pp.

Liu, D.S., Kelly, M. and Gong, P., 2006. A spatial-temporal approach to monitoring forest disease spread using multi-temporal high spatial resolution imagery. Remote Sensing of Environment, 101(2): 167-180.

Lohani, V. and Loganathan, G., 1997 An early warning system for drought management using the Palmer drought index Journal of the American Water Resources Association 33(6): 1375-1386

Lohani, V.K., Loganathan, G.V. and Mostaghimi, S., 1998. Long-term analysis and short-term forecasting of dry spells by Palmer Drought Severity Index. Nordic Hydrology, 29(1): 21-40.

McKee et al., 1993. The Relationship of drought Frequency and Duration to time scales, Eighth Conference on Applied Climatology,. Department of Atmospheric Science, Anaheim, California.

Melgani, F. and Serpico, S.B., 2003. A Markov random field approach to spatio-temporal contextual image classification. Ieee Transactions on Geoscience and Remote Sensing, 41(11): 2478-2487.

National Drought Mitigation Center, 2006. What is drought, SPI. National Drought Mitigation Center, USA.

Peters, A.J. et al., 2002. Drought monitoring with NDVI-based standardized vegetation index. Photogrammetric Engineering and Remote Sensing, 68(1): 71-75.

Rundquist, B., C. , Harrington, J.A. and Goodin, J.D.G., 2000. Mesoscale Satellite Bioclimatology. The Professional Geographer, 52(2).

Seiler, R., Kogan, F. and Sullivan, J., 1998. AVHRR-based vegetation and temperature condition indices for drought detection in Argentina Remote Sensing: Inversion Problems and Natural Hazards Advances in Space Research 21(3): 481-484.

Sen, Z., 1998 Probabilistic formulation of spatio-temporal drought pattern Theoretical and applied climatology, 61(3-4): 197-206

Singh, R.P., Roy, S. and Kogan, F., 2003. Vegetation and temperature condition indices from NOAA AVHRR data for drought monitoring over India. International Journal of Remote Sensing, 24(22): 4393-4402.

Smakhtin, V.U. and Hughes, D.A., 2004. Review, Automated Estimation and Analyses of Drought Indices in South Asia. International Water Management Institute.

Solberg, Schistad, H. and Anne., 2004. Flexible nonlinear contextual classification
Pattern Recognition Letters 25(13): 1501-1508

Solberg, A.H.S., Taxt, T. and Jain, A.K., 1996. A Markov random field model for classification of multisource satellite imagery. Ieee Transactions on Geoscience and Remote Sensing, 34(1): 100-113.

Steinemann, A., 2003 Drought indicators and triggers: A stochastic approach to evaluation Journal of the American Water Resources Association 39(5): 1217-1233

Thenkabail, P.S., Gamage, N., M.S.D. and Smakhtin, V.U., 2004. The Use of Remote Sensing Data for Drought Assessment and Monitoring in Southwest Asia. 85, International Water Management Institute, Colombo.

Tso, B. and Mather, P., 2001. Classification methods for remotely sensed data. Taylor and Francis.

Tso, B. and Olsen, R., 2005. A contextual classification scheme based on MRF model with improved parameter estimation and multiscale fuzzy line process Remote Sensing of Environment, 97(1): 127-136

Tucker, C., 1989 Comparing SMMR AND AVHRR data for Drought Monitoring International Journal of Remote Sensing 10(10): 1663-1672

Wan, Z., Wang, P. and Li, X., 2004. Using MODIS Land Surface Temperature and Normalized Difference Vegetation Index products for monitoring drought in the southern Great Plains, USA. International Journal of Remote Sensing, 25(1): 61-72.